ANALYSIS OF HEAT TRANSFER ENHANCEMENT IN CHANNEL FLOW THROUGH FLOW-INDUCED VIBRATION

Siva Kumar Kota

Thesis Prepared for the Degree of

MASTER OF SCIENCE

UNIVERSITY OF NORTH TEXAS

December 2017

APPROVED:

Weihuan Zhao, Major Professor
Mark Wasikowski, Committee Member
Xiaohua Li, Committee Member
Kuruvilla John, Chair of the Department of Mechanical and Energy Engineering
Costas Tsatsoulis, Dean of the College of Engineering
Victor Prybutok, Dean of the Toulouse Graduate School

Kota, Siva Kumar. *Analysis of Heat Transfer Enhancement in Channel Flow through Flow-Induced Vibration*. Master of Science (Mechanical and Energy Engineering), December 2017, 47 pp., 5 tables, 26 figures, 39 numbered references.

In this research, an elastic cylinder that utilized vortex-induced vibration (VIV) was applied to improve convective heat transfer rates by disrupting the thermal boundary layer. Rigid and elastic cylinders were placed across a fluid channel. Vortex shedding around the cylinder led to the periodic vibration of the cylinder. As a result, the flow-structure interaction (FSI) increased the disruption of the thermal boundary layer, and therefore, improved the mixing process at the boundary. This study aims to improve convective heat transfer rate by increasing the perturbation in the fluid flow. A three-dimensional numerical model was constructed to simulate the effects of different flow channel geometries, including a channel with a stationary rigid cylinder, a channel with a elastic cylinder, a channel with two elastic cylinders of the same diameter, and a channel with two elastic cylinders of different diameters. Through the numerical simulations, the channel maximum wall temperature was found to be reduced by approximately 10% with a stationary cylinder and by around 17% when introducing an elastic cylinder in the channel compared with the channel without the cylinder. Channels with two-cylinder conditions were also studied in the current research. The additional cylinder with the same diameter in the fluid channel only reduced the surface wall temperature by 3% compared to the channel without any cylinders because the volume of the second cylinder could occupy some space, and therefore, reduce the effect of the convective heat transfer. By reducing the diameter of the second cylinder

by 25% increased the effect of the convection heat transfer and reduced the maximum wall temperature by around 15%. Compared to the channel with no cylinder, the introduction of cylinders into the channel flow was found to increase the average Nusselt number by 55% with the insertion of a stationary rigid cylinder, by 85% with the insertion of an elastic cylinder, by 58% with the insertion of two cylinders of the same diameter, and by approximately 70% with the insertion of two cylinders of different diameters (the second cylinder having the smaller diameter). Furthermore, it was also found that the maximum local Nusselt number could be enhanced by around 200%-400% at the entrance of the fluid channel by using the elastic cylinders compared to the channel without cylinders.

ACKNOWLEDGEMENTS

Many people who helped me throughout this journey. My advisor, Dr. Weihuan Zhao, was invaluable. I would like to thank her for giving me the opportunity to study under her, and for providing me assistance with her breadth of knowledge in the fields of both heat transfer and computational fluid dynamics. She was always willing to provide insight when I needed it.

I would also like to thank committee members Dr. Mark Wasikowski and Dr. Xiaohua Li for their support.

I am very grateful for the assistance provided by Dr. Suresh and Dr. Sujan. Without them, this work would not have been possible. I would also like to thank my colleagues and friends, Devin, Robert Richard, Raghav Bandi, Prasanna, and Vishnu for their companionship and assistance during hard times. I would like to thank my roommates and friends for their good company.

I would also like to extend my gratitude to Robbin Shull, MEE lab manager for providing everything that helped me to complete this thesis.

Last but not least, I am forever grateful to my parents and family for all the love and support they have given me in my life, and for the opportunity they provided me in attending university. I am equally thankful for the love and support of my grandfather, Bade Manmadha Rao, who helped a lot with my master's education.

TABLE OF CONTENTS

Page

LIST OF TABLES

Page

LIST OF FIGURES

Page

NOMENCLATURE

C_p	Heat capacity at constant pressure (Specific heat) (J/ Kg·K)
D	Diameter of the cylinder(m)
D1	Reduced diameter of the cylinder(m)
E	Modulus of elasticity (Pa)
F_v	Volumetric boundary force (N/m^3)
H	Height of the channel(m)
k	Thermal conductivity (W/m·K)
L	Length of the channel(m)
L1	Distance between the channel entrance and the center line of the cylinder(m)
L2	Distance between the two cylinders(m)
Nu	Nusselt number
P	Pressure (Pa)
Q	Heat source (W)
Re_D	Reynolds number in the fluid channel
Re_{Dh}	Reynolds number around the cylinder
T	Temperature (K)
T_{inlet}	Inlet temperature (^{0}C)
T_{wall}	Wall temperature (^{0}C)
U_{fluid}	Fluid velocity field (m/s)
U_{in}	Fluid velocity(m/s)
U_{solid}	Solid object displacement (m)

W1 Length of the cylinder (m)

W Width of the channel(m)

Greek Symbols

ρ_f Density of the fluid(kg/m^3)

ρ_s Density of the elastic material (kg/m^3)

σ Stress (N/m^2)

CHAPTER 1

INTRODUCTION

1.1 Background

Various techniques to enhance convective heat transfer have been investigated and applied with in the industry as well as in daily life, including two-phase flow i.e, convection with a phase change. These techniques are used in vortex generators, nanofluids, fins, and fluid-structure interactions. According to Bergles et al [23] heat transfer enhancement techniques are divided into two groups: active techniques, and passive techniques. Active techniques require external power sources; jet impingement, fluid vibration, mechanical aids, surface vibrations, suction and electrostatic fields have been used to enhance the convective heat transfer coefficients. Passive techniques require geometrical modifications to enhance the convective heat transfer, such as the use of a fin structure to improve the heat transfer surface areas, surface modifications to enhance the heat transfer coefficient, and displaced insert devices. Compound techniques were also used by combining active and passive techniques to improve heat transfer performance by enhancing thermal boundary layer disruption.

In 2013 Léal et al. [24] briefly discussed the techniques for heat transfer enhancement between the solid wall and a fluid for both single-phase as well as two-phase systems. They briefly explained commonly used passive techniques to enhance the heat transfer performance of heat exchangers by increasing the heat exchange surface area.

The surface coating used in the micron scale method [24] could help to improve convective heat transfer by increasing turbulence in the boundary layer, therefore, disrupting the thermal boundary layer. Kakac et al. [25] found that adding a nano-fluids suspension to the fluid could help to increase thermal conductivity and change the viscosity and density of the fluid, and therefore, enhance convective heat transfer performance. Bontemps et al. [26] and Miscevic et al. [27] found that inserting external fins [26] and, porous [27] and finned plates into the flow increased the heat transfer coefficient.

In 2009, Dalkilc et al. [28] reviewed in-tube condensation by inserting external inserts and also emphasized the importance of using hydrocarbons instead of fluorocarbons. Cavilani et al. [29] achieved 140% increase in heat transfer coefficient by using micro-fin-tubes., whereas in 2003, Miyara et al. [30] achieved a 350% increase in heat transfer coefficient by inserting herringbone tubes in the channel flow.

Kumar and Prasad [32] investigated the improvement of heat transfer enhancement in a solar water heater by inserting a twisted tape with twist pitch having the diameter ratio ranging from 3-12 into the tube. The twisted-tape generated turbulency with swirlness inside the flow. The researchers found that the heat transfer rate would be increased by reducing the twist ratio. However, this would result in an increase of the pressure drop in the solar water heater.

Promvogue [33] increased convective heat transfer in a uniform heat flux tube by using conical rings as a turbulator mounted on the tube. This resulted in the improvement of Nusselt number of 197%, 333% and 237% in the turbulent flow for converging conical

ring array (CR), diverging conical ring array (DR) and converging-diverging conical ring arrays (CDR) respectively.

Promvogue et al. [34] presented the effect of free-spacing snail entry together with conical nozzle turbulators on turbulent heat transfer and friction characteristics in a uniform heat flux tube. Observed with the application of C-nozzles and free spacing snail entry resulted in, higher enhancement rate and frictional loss at lower pitch values compared to larger pitch values at constant Reynold number.

Gunes et al. [35] investigated the heat transfer and pressure drop in a turbulent flow regime with the coiled wire inserted tube. The experimental results revealed that the best operating regime in the coiled wire inserted tubes was at low Reynolds number turbulent flow regime.

Sheikholeslami et al. [31] reviewed various passive method techniques investigated on coil tubes, roughed surfaces, extended surfaces and swirl flow devices like twisted tape, conical ring, snail entry turbulator, vortex rings and coiled wire. By reviewing various techniques under various flow conditions (Laminar Flow, Turbulent flow), they concluded that wire coil gives better overall performance if pressure drop penalty was considered.

Air has been considered as a heat transfer fluid (HTF) for many applications for decades. The advantages of air as an HTF are that (1) it can be easily accessed, (2) it has low cost, (3) it is not harmful to human health and is friendly to materials under most common conditions, (4) it can be operated under a board temperature range, (5) will not freeze or boil and is non-corrosive, (6) has very low heat capacity and (7) it tends to

leak out of collectors and ducts. However, the transfer performance of air is usually poor due to its low heat transfer coefficients. Therefore, it cannot efficiently remove the heat from the materials or devices. Hence, it is important to find proper techniques for air to enhance its heat transfer performance.

Through introducing elastic cylinders across the air flow in the channel, vortex shedding would be formed around the cylinder. The vortex shedding would cause the vibrations of the elastic cylinder in the flow, which could further increase the vortex generation in the fluid flow. This type of vortex-induced vibration (VIV) can disturb the thermal boundary layer, and therefore, increase the heat transfer performance of the fluid flow [22].

1.2 Objectives

The main objectives of this research are to investigate the heat transfer enhancement of air flow by introducing flow-induced vibration through elastic cylinders in the cross flow. Three-dimensional (3-D) flow-structure interaction (FSI) simulations were conducted for the air flow under various cylinder arrangements in the fluid channel by COMSOL Multiphysics. Five different fluid channel geometries have been studied, including the channel without cylinders (the baseline),the channel with stationary rigid cylinder, the channel with an elastic single cylinder, the channel with two elastic cylinders of the same diameter, and the channel with two elastic cylinders of different diameters. Through the numerical simulations, the enhancement of the heat transfer performance of air flow by the vibrating cylinder will be determined.

1.3 Impact of Research

The research will improve the heat transfer rate of air flow to make air a more effective HTF in heat exchange applications. To enhance heat transfer coefficient, air can be used as the working fluid in many fields, i.e., vehicle cooling system, the dry-cooling system in power plants, solar water heating systems, heat exchangers, solar thermal energy applications, nuclear power plants and air fueled condensing systems, etc. Furthermore, this research is using a novel, elastic method to enhance the heat transfer performance without additional external power source requirement. Therefore, it can be easily applied and reduce the costs of the cooling system.

CHAPTER 2

LITERATURE REVIEW

In this chapter, various perturbation methods to enhance the thermal boundary disruption have been investigated by other scientists and researchers to increase the heat transfer rates of HTFs, and therefore, improve the cooling capacity of fluid flow is discussed.

2.1 Flow Perturbation Methods

The cooling capacity of channel flow increases proportionally with thermal boundary disruption. There are several methods there to hamper the performance of the thermal boundary layer thereby increasing heat transfer enhancement [1]. Vortex induced heat transfer performance is implemented by active methods. An early study that elaborately explains the active methods which were used to enhance the vortex generations i.e., Johnson et al. [3] first studied the vortex generator impact on the heat transfer enhancement in 1969. They observed that, vortex generators improved the local Nusselt Number as much as 200%,but overall heat transfer results were decreasing.

Kataoka et al. [4] briefly addressed the mechanisms of local enhancement. They addressed the local behavior for an inner rotating cylinder with the outer stationary cylinder with an imposed axial velocity in the annulus. This arrangement results in a system of axially adverted Taylor vortices.

Streamline vortices occur when flow suddenly encounters the surface element protruding into the surface layer. Sedney [5] reviewed the effects of small protuberance

on the boundary layer flows. In this, he explained the disturbances caused by arranging protuberance in the laminar and turbulent flow.

Shakaba et al. [37] experimentally explained the interaction between the longitudinal vortex to the turbulent boundary layer. In this, the measurements indicated that the vortices were very persistent.

The association of flow and heat transfer in Junction vortex systems is deliberately explained by Baker [6]. In this, the horseshoe vortex formed around the base of the cylinder by separating laminar boundary layer has been experimentally investigated. Pressure distribution between steady and unsteady vortex systems has been measured and the complex oscillatory behavior of the horseshoe vortex systems has been observed.

The passive vortex heat transfer was studied in the mid-1970s by Edwards and Alker [2]. In this study, three-dimensional surface protuberance conceded to improve the convective heat transfer to gases. A row of cubes and a row of vortex generator blades are used in six different arrangements for the observation. It was discovered that cubes produce the highest local improvement.

Furthermore, placing winglet vortex generators into lowered fin surface increase the swirling motion of the winglet, reduces the boundary layer thickness and finally increase the heat transfer enhancement. Huisseune et al. [10] studied the effect of punching delta winglet vortex generators into the louvered fin surface. The delta winglets reduce the size of the tube wakes. They cause a swirling motion in the vortices, hot air is removed from the tube wake to the mainstream and vice versa. Induced wall-normal

flow reduces the boundary layer thickness thereby enhance heat transfer. Finally, wake zone size is reduced because of the delay in flow separation from the tube surface.

He et al [11] studied the heat transfer enhancement by punched winglet-type vortex generator arrays in fin and tube heat exchangers. The arrays are composed of two delta-winglet pairs with two layout modes of continuous and discontinuous winglets. The winglets were placed at different attack angles and layouts and the heat transfer performance was observed. Heat transfer coefficient and pressure drop increase with the increase in attack angles for side arrangements.

Jagannatha et al. [12] used the synthetic jet in the microchannel to observe the behavior of the fluid flow and heat transfer enhancement. They observe the behavior of the fluid flow with different parametric conditions and found out pulsating jet generate 4.3 times the heat dissipation compared to the channel flow without pulsating jet within the tested parametric range.

Yu et al. [13] enhanced the heat transfer in air-cooled heat sinks using piezoelectrically driven alligators and synthetic jets. In this, they observed the combination of agitator and synthetic jets raises the heat transfer coefficient of the channel flow by 82.4% compared to the channel with the flow.

Li Hung-Yi and Chen Kuan-Ying [14] used impinging jets to enhance the thermal performance by increasing Reynolds number and reducing thermal boundary thickness. Chao Shung-Ming et al. [15] analyze the changes in surface temperature with the introduction of the shield in the heat sink and observe the changes in thermal boundary thickness with increase in Reynolds number.

2.2 Fluid-Structure Interaction Methods

Investigations on the fluid-structure interactions have been conducted in various aspects in the last decades. Cheng et al. [7] explained the perturbed interaction between vortex shedding and induced vibration. In this, they briefly described the technique to create vortex shredding from a bluff-body and VIV with a control flow and structural vibration. A.L.C. Fujarra et al [8] illustrated about the Vortex-induced vibration of a flexible cantilever in fluid flow. In this cylinder, the cantilever is constructed by using a rubber but within the structure was made up of aluminum plate to get maximum flexibility to the flow.

In 2011, Martin D Griffinth et al [9] presented the investigation of flow past a circular cylinder in the two-dimensional channel of varying width. In this experiment, the flow from the cylinder varying with the Reynolds number and blocking ratio. Vortex behavior is steady with the low Reynolds number values whereas it varies with the increase in Reynolds number.

The structural interaction between the vortex induced vibration and fluid fields are widely used in multiple applications. Yamato C T et al [16] observed the vortex-induced vibrational behavior of flexible cylinder under the influence of current and shear flow. In this process, hydrodynamic forces are applied on the flexible cylinder by using discrete vortex method and the results further compared with the experimental results obtained by quasi-steady theory proposed by Bearman et al in 1984 [39]. In addition to this, it is further compared to the practical experimental results observed by Fujarra [8] involving cantilever flexible cylinder immersed in the current.

The effect of critical damping and mode of vibration with the application of dynamical forces on the mounted rigid cylinders were observed. The importance of critical mass, vorticity and, the relationship between vorticity and force clearly explained by Williamson and Govardhan [17] in 2004.

The circular cylinder behavior between the two parallel plates was clearly observed by Singha et al [18] with the varying of Blocking ratio and Reynolds number. In this experiment, the rise of vortex shedding regime is less when the cylinder is near to the channel walls.

The above researchers discussed the interaction between the fluid flow with the cylindrical objects or cantilever beams. They mostly consider the interaction between the structures and fluid flow with the varying of conditions like changing blocking ratio and change in mass and vorticity. But they did not give most priority to the convective heat transfer enhancement of the channel flow with the fluid-induced vibration.

Few researchers observed the vortex induced vibration with the walls and enhance the heat transfer performance. In 2004, Fu W-S and Tong B-H [19] studied the performance of an oscillating cylinder on the heat transfer from the heated blocks in a channel flow. In this study, a cylinder was placed in the channel flow with four heating blocks with a temperature higher than the fluid temperature. The results explained, remarkable heat transfer enhancement occurred at the lock-in region and the increase in Reynolds number increases the heat transfer rate.

Thermal performance of the cooling systems can be increased by varying the geometric modifications of the system. Placing objects in the channel flow would change

the flow and thereby increase the thermal performance and increase the heat transfer coefficient. C Bayram et al. [20] use this concept and thereby investigate the heat transfer enhancement in the uniformly heated slot channel due to vortices from the transversely oscillating adiabatic circular cylinder. In this, they particularly observe the performance at fixed Reynolds number Re=100 in the straight channel and in the stationary channel. They observe the increase in transverse oscillations and heat transfer coefficient in the straight flow than the stationary channel flow.

In 2012, Beskok Ali et al [21] investigated the heat transfer enhancement in a straight channel via a rotating oscillating adiabatic cylinder. In this, they explored the changes in rotation angle and frequency influence on thermal performance in varying latter in a range of the lock-in-regime and all results based on simulation is unsteady incompressible Navier-Stokes and energy equations.

Shi et al. [22] enhanced heat transfer by using vortex induced vibration in the channel flow by using a 3-Dimensional rectangular model. In this, a flexible cylinder is placed at the center line of a rectangular channel. This flexible channel disturbs the thermal boundary layer by fluid-structure interaction thereby increasing the mixing process inside the channel to improve heat transfer performance. The performance enhanced for three different cases in the channel, i.e, clean channel, a channel with fixed cylinder and channel with the flexible cylinder. Low inlet velocities applied at the inlet with Reynolds number varying from (84-168). At 168 Reynolds number, the channel with flexible cylinder observes 214% and 54% increment in the average Nusselt number as opposed to the clean channel and the channel with fixed cylinder respectively.

2.3 Motivation For This Study

Although much research has been focusing on using the VIV method to enhance the heat transfer performance of fluid flow, the vibration of the solid was usually caused by an external power source to make the object vibrate periodically, which made the cooling system complex. Therefore, our research is studying the use of the elastic cylinders in the fluid flow to enhance the heat transfer performance, especially for the HTF with poor heat transfer such as air. The vibration of the solid object was caused by the vortex shedding, without an additional external power source to agitate the cylinder. This technique could simplify the cooling system configuration for the devices, and therefore, reduce the costs.

CHAPTER 3

MATHEMATICAL MODEL AND NUMERICAL METHODS

3.1 Modeling Geometries

Numerical simulations were conducted for four cases of different fluid channel geometries:

- Case 1: The fluid channel without cylinders
- Case 2: The fluid channel with single stationary rigid cylinder
- Case 3: The fluid channel with single elastic cylinder
- Case 4: The channel with two elastic cylinders of the same diameter
- Case 5: The channel with two elastic cylinders of different diameters (the second cylinder diameter reduced by 25%)

Air was used as the HTF in the channel. Through the FSI simulations, heat transfer and fluid dynamics performances of various geometries of cooling channels were analyzed.

3.1.1 The Single-Cylinder Channel

As shown in Figure 3.1, a cylinder was placed in the cross flow in the channel. The dimensions of the fluid channel were illustrated in Table 3.1. The cylinder was placed at 0.2 m from the entrance of the channel. The cylinder was fixed at the two ends. The air flow inlet velocity was 1 m/s. The inlet temperature of the air was maintained at a constant temperature of 20°C. Constant heat rate of 100 W was applied on the top surface of the channel. Because of the symmetric geometry of the channel, the simulation was conducted only for half of the channel geometry to save computational times, as shown in Figure 3.1.

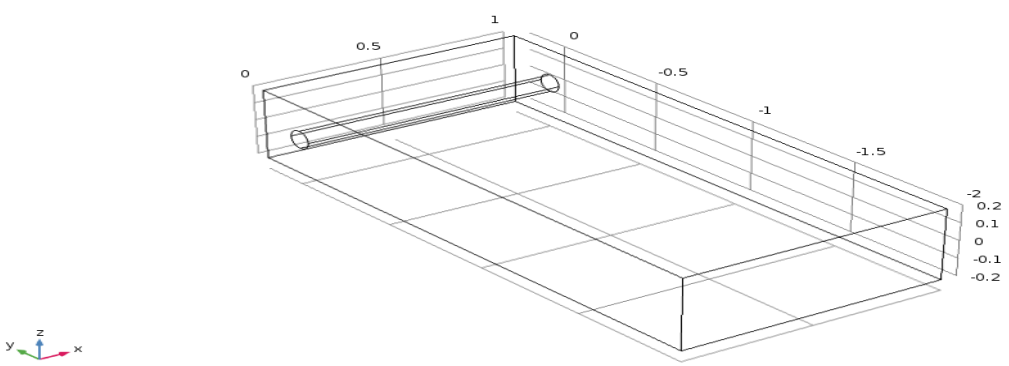

(a): 3-D overall view (units in meters)

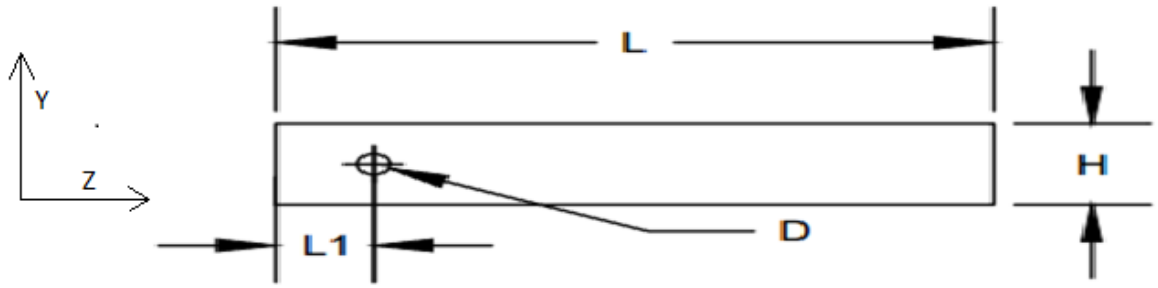

(b): Y-Z plane (units in meters)

Figure 3.1: 3-dimensional geometry for the air flow channel with single cylinder inside, (a) 3-D overall view, (b) Y-Z plane

Table 3.1: Dimensions of the Cylinder and Channel (unit in meters)

Length of the channel (L)	2.2
Width of the channel (W)	2.0
Height of the channel (H)	0.4
Diameter of the cylinder (D)	0.1
Reduced diameter of the cylinder (D1)	0.075
Length of the cylinder (W1)	2.0
Distance between the channel entrance and the centerline of the cylinder (L1)	0.2
Distance between the two cylinders (L2)	1.0

3.1.2 The Channel with Two Cylinders of the Same Diameter

Two cylinders with the same diameter were placed in the cross flow in the channel as shown in Figure 3.2. The distance between the two cylinders was 1m as shown in

Figure 3.2. The two ends of both cylinders were fixed at the channel wall. The diameter of the two cylinders was 0.1 m. The dimensions of the fluid channel were displayed in Table 1 above. The heat flux rate applied on the top surface of the channel was also 100 W.

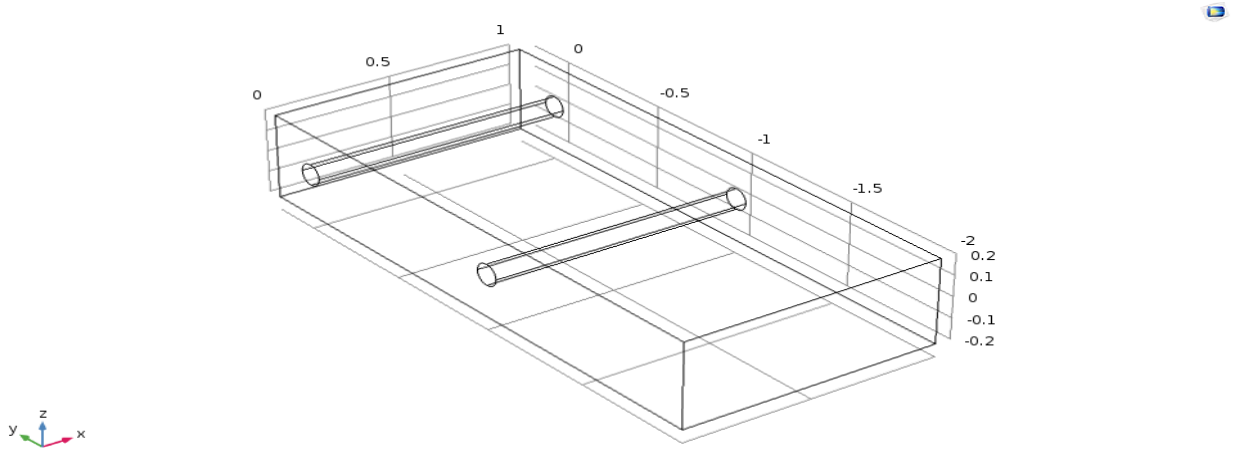

(a) 3-D overall view of the two cylinders with the same diameter (units in meters)

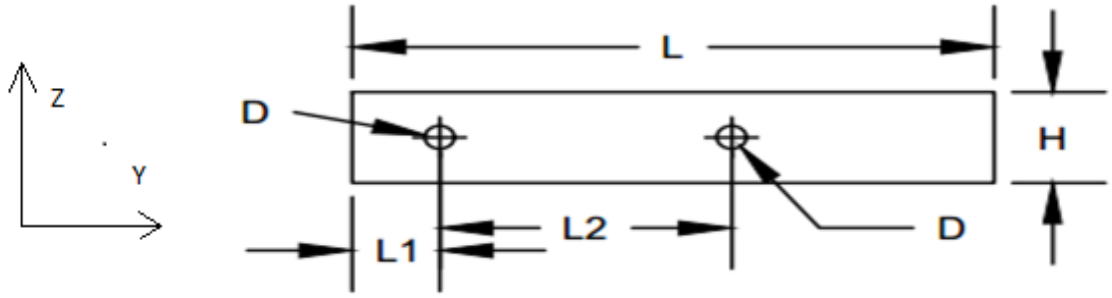

(b) Y-Z plane of the two cylinders with same diameter (units in meters)

Figure 3.2: 3-dimensional geometry for the air flow channel with two cylinders of same diameter inside, (a) 3-D overall view (b) Y-Z plane

3.1.3 The Channel with Two Cylinders of Different Diameters

In this model, the second cylinder diameter is reduced by 25% i.e., 0.075 m. All the other conditions of the cylinders and the fluid channel were the same as Table 3.1 and Figure 3.2.

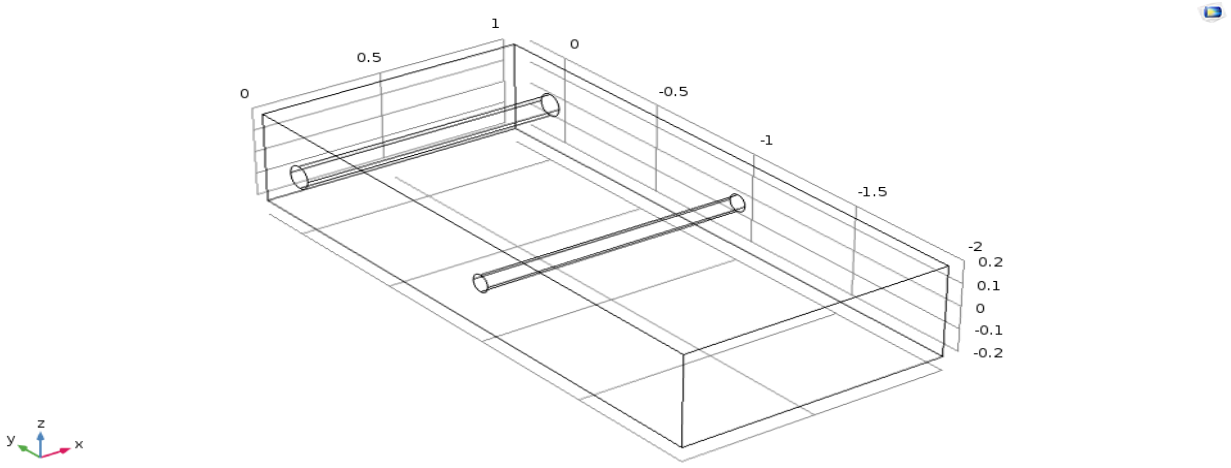

(a) 3-D overall view of the two cylinders with the different diameter (units in meters)

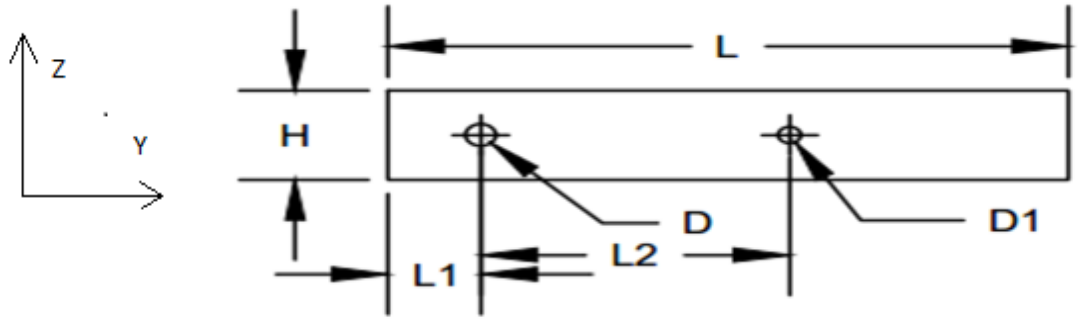

(b) Y-Z plane of the two cylinders with different diameter (units in meters)

Figure 3.3: 3-dimensional geometry for the air flow channel with two cylinders of different diameter inside, (a) 3-D overall view (b) Y-Z plane

The cylinder in the channel was made by the linear elastic material. The material properties of the cylinder are illustrated in Table 3.2. The HTF air properties are displayed in Table 3.3.

Table 3.2: Material Properties of the Cylinders

Density	2343.8 (kg/m^3)
Poisson's ratio	0.3
Young's modulus	0.41 (MPa)
Thermal conductivity	0.5 (W/m·K)
Specific heat	1675 (J/kg·K)

Table 3.3: Properties of Air at 25°C

Dynamic viscosity	1.84×10^{-5} (kg/m·s)
Density	1.18 (kg/m^3)
Thermal conductivity	0.026 (W/m·K)
Specific heat	1004.9 (J/kg·K)

For air inlet velocity of 1m/s, the Reynolds number generated in the duct was around $Re_{Dh} = 6.7\times10^4$. Whereas, the Reynolds number around the cylinder at the inlet of the duct was around $Re_D = 6618$.

3.2 Numerical Model

3.2.1 Fluid-Structure Interaction Model

The incompressible fluid was considered in the simulation model. The momentum equation and continuity equation are expressed in Equations (1) and (2), respectively.

The momentum equation:

$$\rho_f \frac{\partial \mathbf{U}_{fluid}}{\partial t} + \rho \mathbf{U} \cdot \nabla \mathbf{U}_{fluid} = -\nabla P + \mu \nabla^2 \mathbf{U}_{fluid} \quad \text{.... (1)}$$

The Continuity equation:

$$\nabla \cdot \mathbf{U}_{\mathbf{fluid}} = 0 \quad \text{..... (2)}$$

where ρ_f denotes density of the fluid (air) (kg/m^3), U_{fluid} is the velocity field (m/s), μ is the viscosity, p is the pressure (Pa).

3.2.2 Heat Transfer Model

In the heat transfer model, the thermal equation was expressed in Equation (3):

$$\rho_f C_p \frac{\partial T}{\partial t} + \rho C_p \mathbf{U}_{fluid} \cdot \nabla T = k \nabla^2 T \qquad \text{..... (3)}$$

Where C_P is the specific heat (J/kg·K), k is the thermal conductivity (w/m·K), T is the temperature (K), t is the time in (s), ∇T is temperature gradient and Q is the heat source (w/m^3).

3.2.3 Solid Model

Equation 4 explains the energy equation for solid model,

$$\rho_s \frac{\partial^2 \mathbf{U}_{solid}}{\partial t^2} - \nabla \cdot \sigma = F_v \quad \text{..... (4)}$$

where ρ_s is the density of the cylinder (elastic material) (kg/m^3), $.\sigma$ is the stress (N/m^2) and F_v is the volumetric body force (N/m^3). Here F_V was assumed to be zero. The body force was neglected in the current simulation.

3.3 Boundary Conditions

3.3.1 Fluid Flow

The flow inlet velocity was maintained at 1 m/s. The flow outlet condition was considered as the constant atmospheric pressure.

The other channel walls were considered as no-slip boundary condition

$$\mathbf{U}_{fluid} = 0 \quad \text{..... (5)}$$

3.3.2 Solid Model

The interface boundaries between the air flow and the elastic cylinder are

expressed in Equations (6) – (8) to express the interaction between fluid and structure.

$$\mathbf{U}_{fluid} = \mathbf{U}_{w} \quad \text{..... (6)}$$

$$\mathbf{U}_{w} = \frac{\partial \mathbf{U}_{solid}}{\partial t} \quad \text{..... (7)}$$

$$\boldsymbol{\sigma} \cdot \mathbf{n} = 0 \quad \text{..... (8)}$$

In here $\boldsymbol{\sigma} = -P\mathbf{I} + \mu\left[\nabla \mathbf{U}_{\mathbf{fluid}} + \left(\nabla \mathbf{U}_{\mathbf{fluid}}\right)^{T}\right]$, whereas $\mathbf{U}_{\mathbf{fluid}}$ is the fluid velocity field (m/s), P is the pressure (Pa) and $\mathbf{I}$ is the identity matrix.

The two ends of the cylinder were fixed at the channel wall:

$$\mathbf{U}_{\mathbf{solid}} = 0 \quad \text{..... (9)}$$

3.3.3 Heat Transfer Model

Uniform heat flux was applied on the top surface of the channel, q = 100 W. The remaining boundaries were assumed to be well insulated and there is no exchange of temperature.

3.4 Mesh Independent Study

The Navier-Stokes equations were solved on a freely moving deformation mesh which contained the fluid domain. The Winslow smoothing [38] was used to get the deformation of the initial shape of the domain. Winslow smoothing generally adapt to smoothing of two-dimensional unstructured meshes using finite difference approach. The moving mesh on the inside of the solid wall of the channel followed the structural deformation.

Various mesh element sizes were studied and compared to get the effective mesh size as well as mesh type to obtain accurate simulation results. For the mesh independent

study, flexible single-cylinder channel geometry was considered for the observation. Figure 3.4 (a) showed the mesh structures for the single-cylinder channel. Figure 3.4(b) displayed the mesh structure around the cylinder in the y-z plane of the fluid channel. There were 66008 domain elements created in the *y-z* plane, which was sufficient for the FSI simulations in the 2-D domain as displayed in Figure 3.4(b). Then, the mesh structure in the *y-z* plane was used and swept in the *x*-direction for the entire 3-D geometry domain.

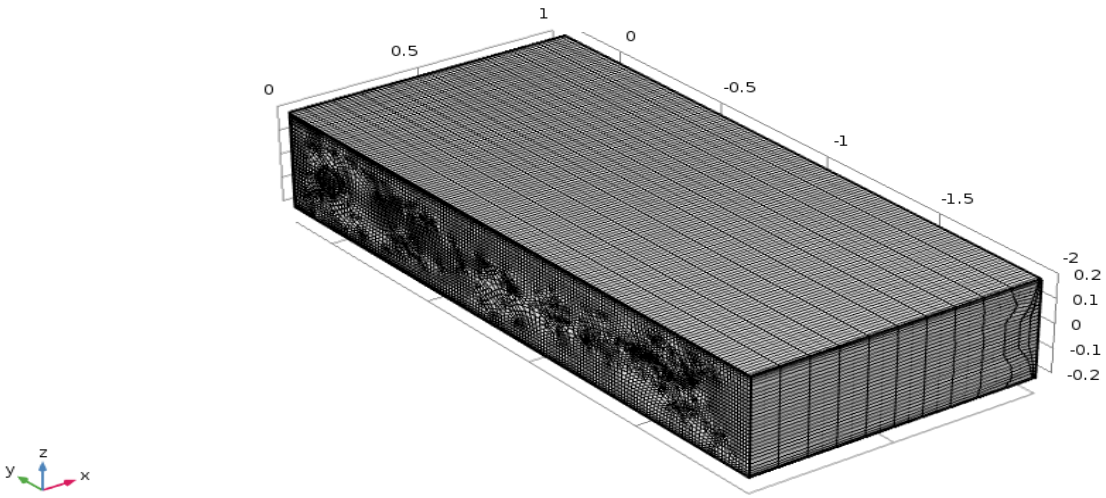

(a) Mesh structure for the 3-dimensional geometry

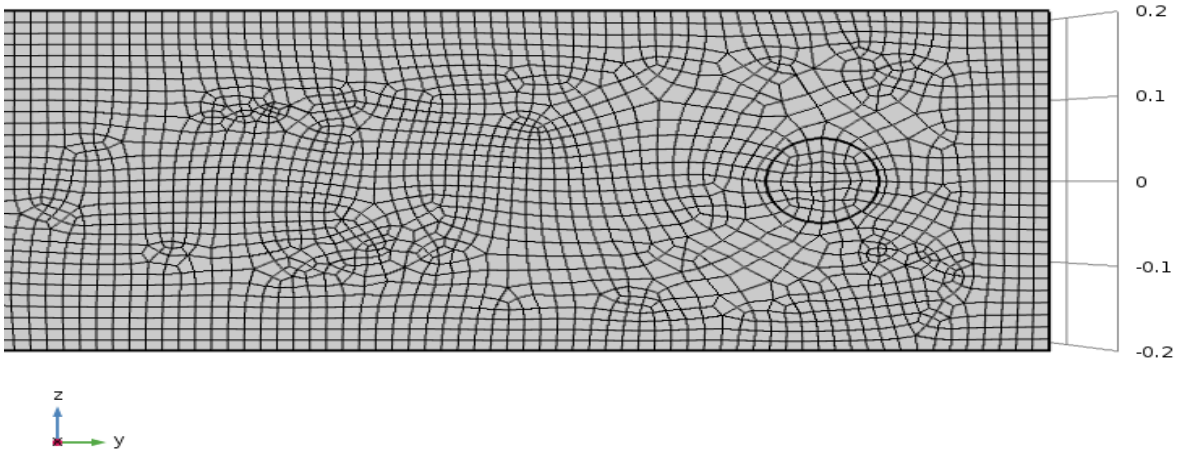

(b) Mesh structure around the cylinder in the fluid channel

Figure 3.4: Mesh structure for the single-cylinder fluid channel model (a) Mesh structure for the 3-dimensional geometry, (b) Mesh structure around the cylinder in the fluid channel

Different numbers of swept layers (i.e., 5, 10 and 20 swept layers) were studied to determine the optimal mesh size for the 3-D FSI simulations. Table 3.4 showed various numbers of mesh elements that were used for the mesh independent study.

Table 3.4: Mesh independent study of the flexible single cylinder with total number of mesh elements

Serial Number	Mesh type	Domain elements	Boundary elements	Edge elements	Total elements
1	5 Swept Layers	39396	13015	816	53227
2.	10 Swept Layers	51100	14060	848	66008
3.	20 Swept Layers	125420	18828	936	145184

Figures 3.5 displayed the simulation results from different numbers of swept layers (illustrated in Table 3.4) for the 3-D geometry. Based on Figure 3.5, the simulation results of the maximum temperature observed were consistent for different mesh sizes (i.e., 5, 10 and 20 swept layers)

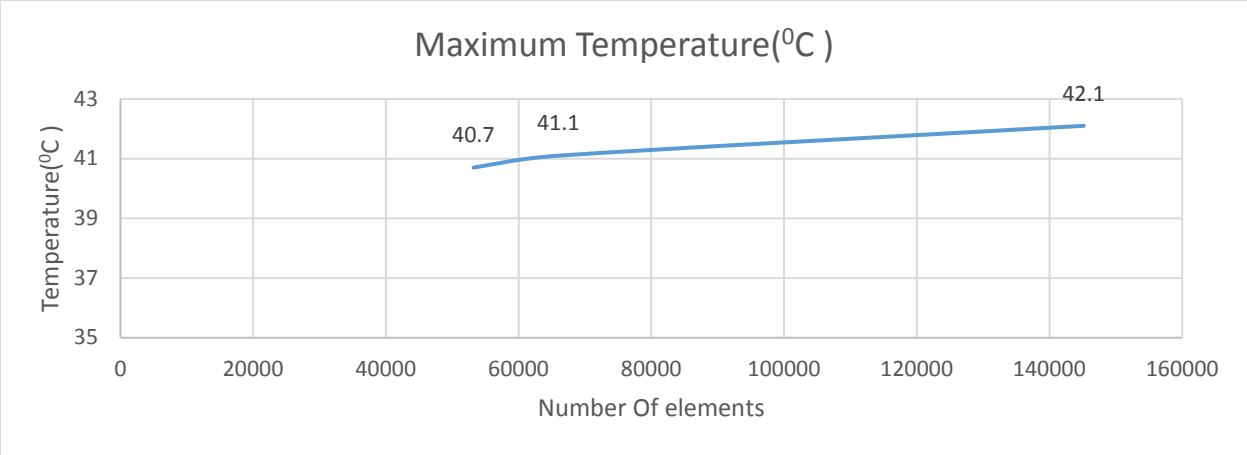

Figure 3.5: Mesh independent study of the single cylinder temperature of the wall (^{0}C) with variable distributions (different mesh elements)

The maximum temperature enhanced for the different mesh elements is shown in Figure 3.5. In this, temperature consistency observed at the 10 distributions. Therefore,

the mesh type shown in Figure 3.5 with 10 swept layers in the *x*-direction was good for the 3-D FSI simulations.

CHAPTER 4

RESULTS AND DISCUSSION

This chapter discusses the behavior of the elastic cylinder with interacting fluid. The lift and drag forces, displacement of the cylinders, the velocity and temperature profiles of the fluid flow, the local and average Nusselt number enhancements in the channel have been investigated in this chapter.

4.1 Velocity Magnitude

To observe the vortices behavior in the channel flow, Figures 4.1-4.4 displayed the velocity contours in the y-z plane of the channel. For all five cases, the inlet velocity was maintained constant at 1 m/s. Figure 4.1 showed that the flow velocity profile in a channel without cylinders. The velocity was maintained at 1 m/s in the flow channel. In Figure 4.2 and Figure 4.3, the maximum velocity magnitude was improved to 1.66 m/s and 1.85 m/s respectively, when placing a rigid cylinder and an elastic cylinder near the inlet of the channel. With the additional cylinder in the fluid channel, the vortex generation behind the cylinder would increase the fluid velocity, and therefore, improve the convective heat transfer rate in the channel. With one rigid cylinder, the vortex generation would decay along the fluid channel as displayed in Figure 4.2. When using the elastic cylinder, it could help to enhance the vortex shedding behind the cylinder (Figure 4.3) and further increase the convective heat transfer in the channel.

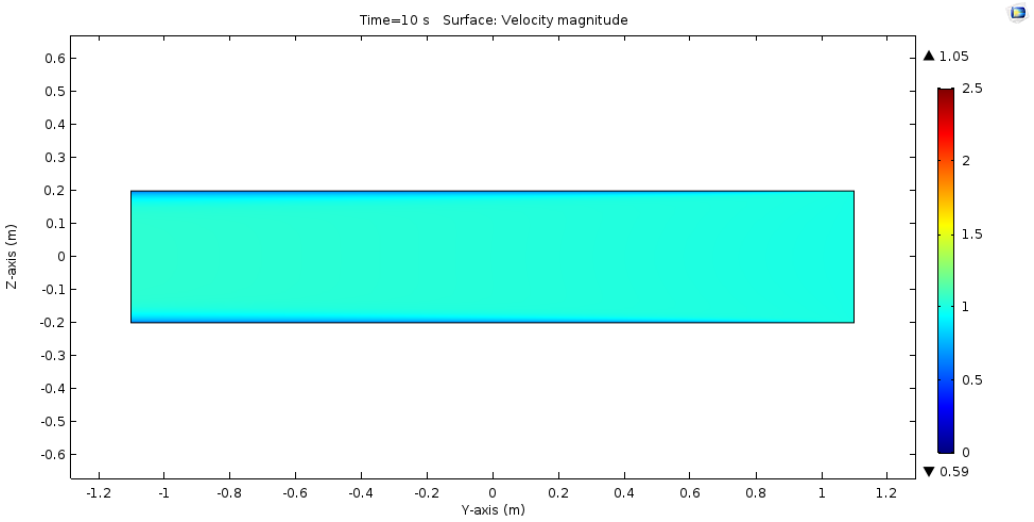

Figure 4.1: Velocity magnitude of fluid flow in the chamber without cylinder

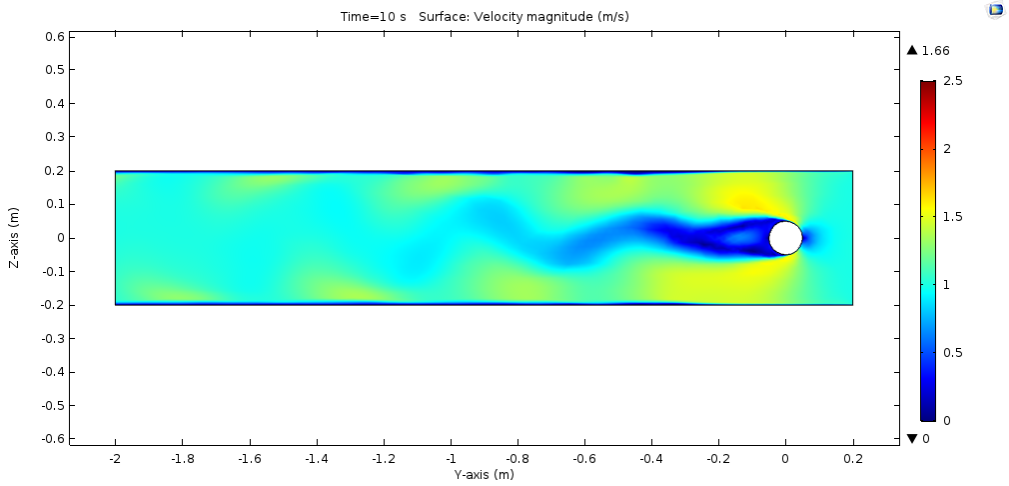

Figure 4.2: Velocity magnitude in the fluid channel with rigid single cylinder

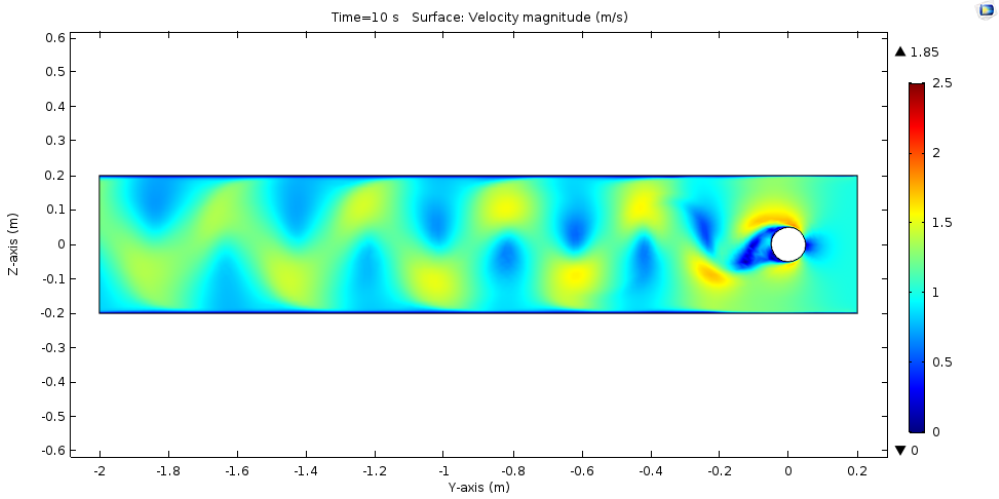

Figure 4.3: Velocity magnitude in the fluid channel with elastic single cylinder

Therefore, a second elastic cylinder was added in the middle of the fluid channel to help re-generate vortex in the fluid, and therefore, overcome the decay of the vortex shedding along the channel. Figures 4.4 and 4.5 displayed the velocity profiles in the fluid channel with two cylinders. Figure 4.4 illustrated the case of a fluid channel with two same-diameter cylinders. The maximum velocity magnitude can reach 1.89 m/s in the channel with the vibration of the two cylinders, which improved the mixing process with the enhanced vortex structure due to the second cylinder in the channel. The maximum velocity magnitude was observed at the rear of the second cylinder with the interaction of the vortices generated by the first cylinder. Figure 4.5 showed a reduced diameter cylinder in the channel. It showed the maximum velocity magnitude of 1.87 m/s at the rear of the second cylinder. The value was slightly lower than the case of the two-same-diameter-cylinder channel due to the reduced diameter of the second cylinder.

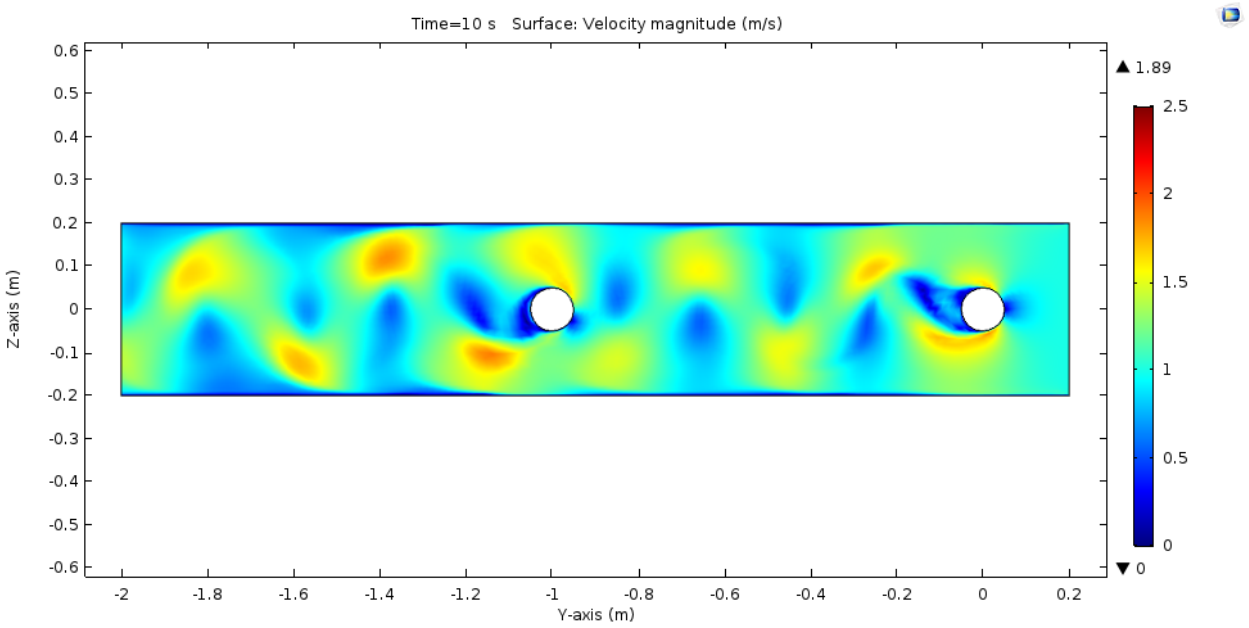

Figure 4.4: Velocity magnitude in the fluid channel with two cylinders of the same diameter

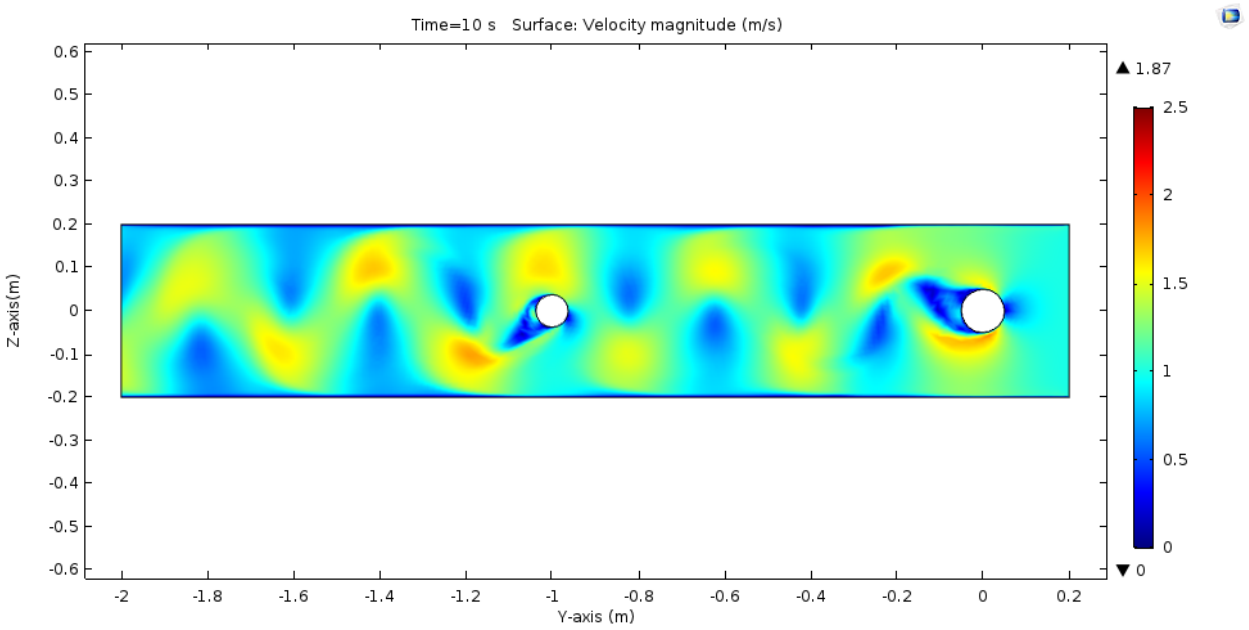

Figure 4.5: Velocity magnitude in the fluid channel with two cylinders of different diameters

4.2 Lift Coefficient

The lift coefficient was calculated by the lift force generated around the cylinder. The lift force was very minor for the stationary rigid cylinder (Figure 4.6) compared with the elastic cylinders (Figures 4.7-4.9). The maximum lift coefficient value for the elastic single cylinder was 0.48 as displayed in Figure 4.7. For the two-same-diameter-cylinder channel, the lift force around the second cylinder was significantly enhanced. The lift coefficient around the second cylinder was around two times higher than the first cylinder near the inlet (Figure 4.8) because of the increased velocity around the second cylinder. The larger velocity circulation around the cylinder would lead to the larger dynamic pressure.

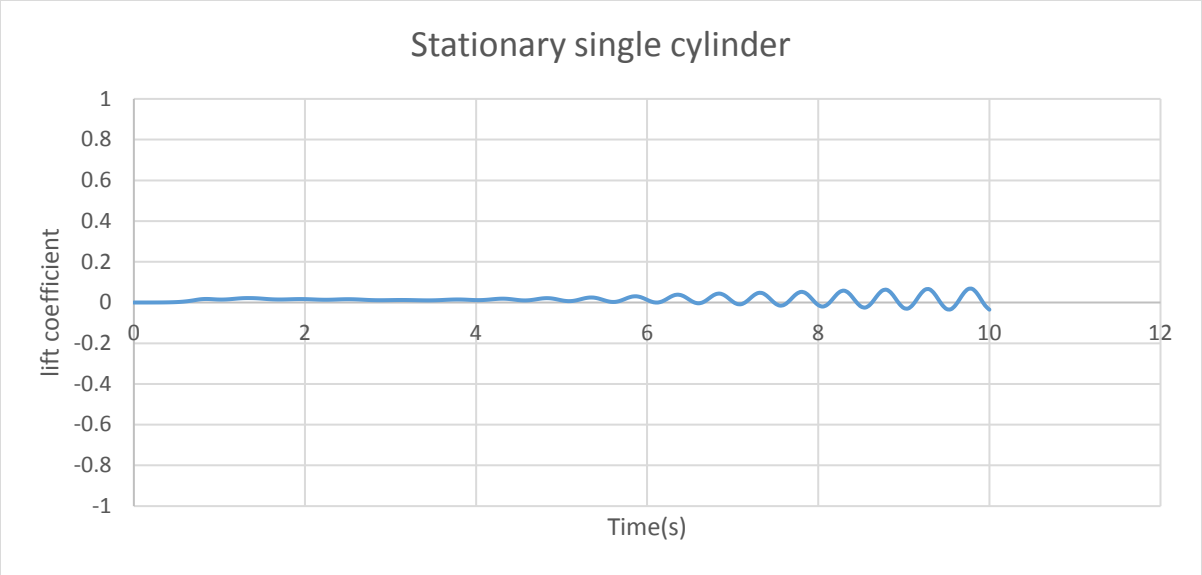

Figure 4.6: Lift coefficient around the cylinder in the channel (for the stationary rigid single cylinder case).

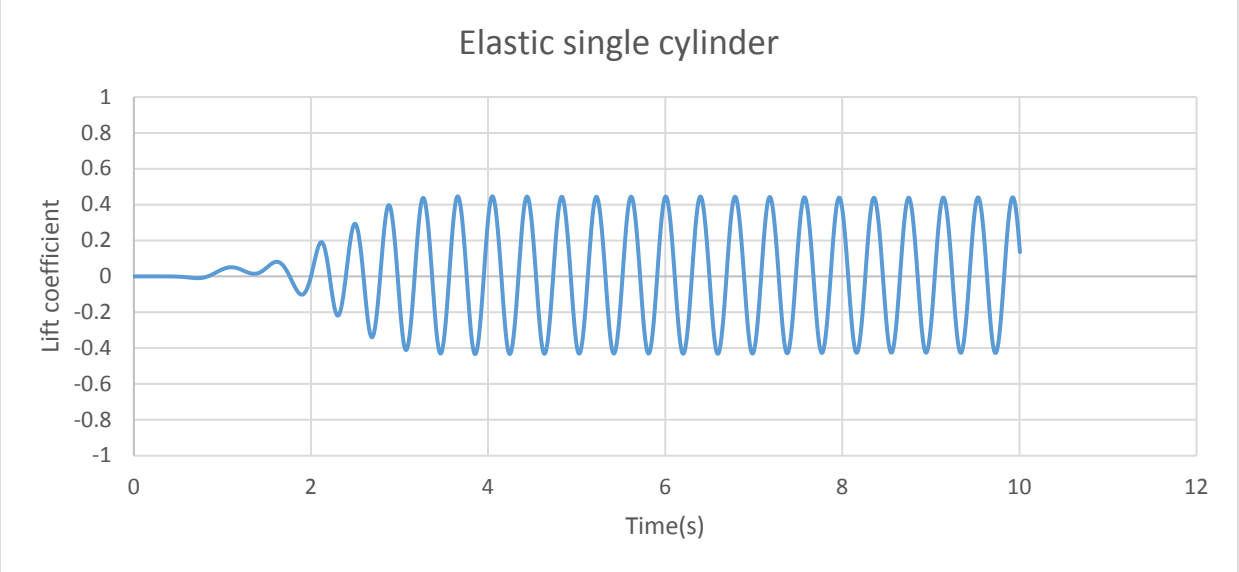

Figure 4.7: Lift coefficient around the cylinder in the channel (for the elastic cylinder case).

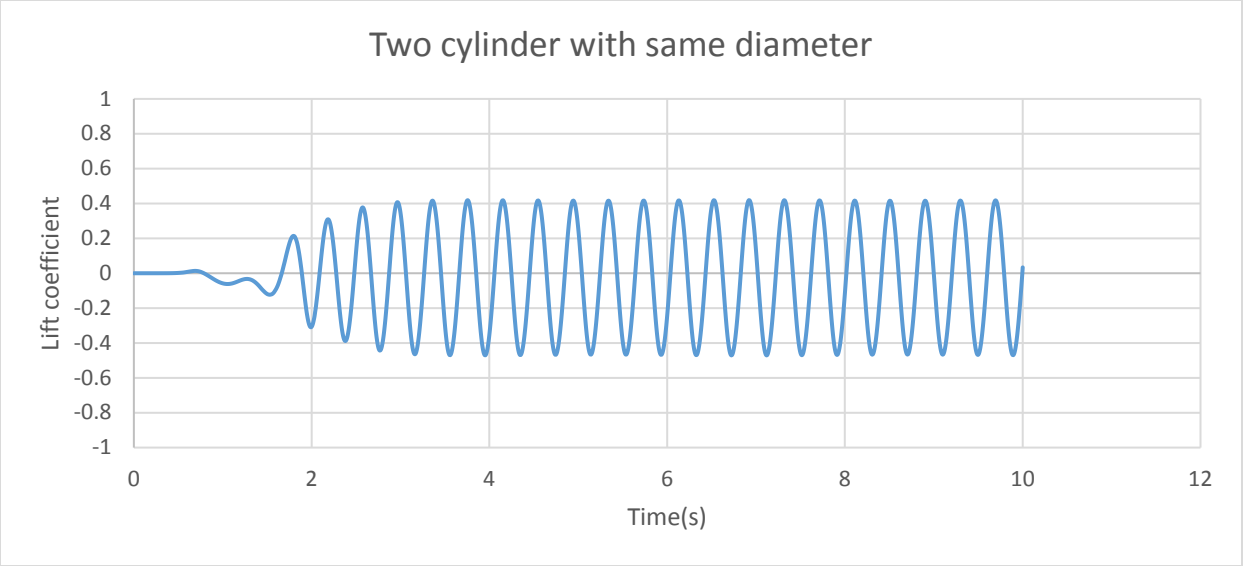

(a) Lift coefficient around the first cylinder (located near the inlet of the channel)

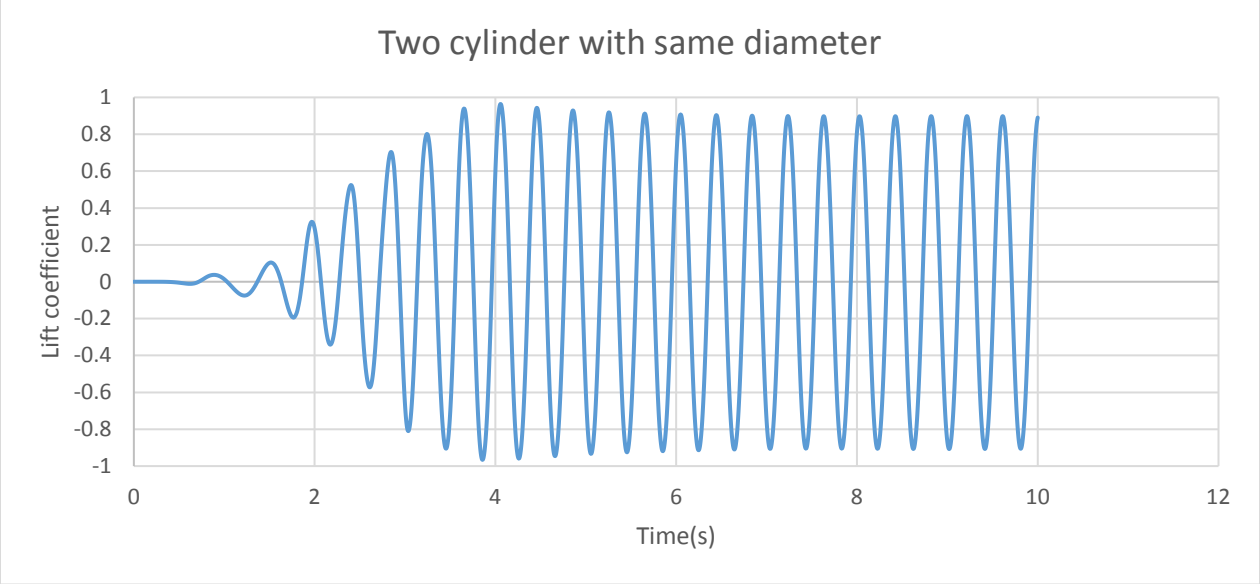

(b) Lift coefficient around the second cylinder (located at the middle of the channel)

Figure 4.8: Lift coefficient around the cylinders in the channel (for the two-same-diameter-cylinder case).

Figure 4.9 showed the lift coefficient for the two-different-diameter-cylinder case.

The lift coefficient values around the first cylinder were similar as the single-cylinder case

and the two-same-diameter-cylinder case (Figure 10 and Figure 11(a)). The lift forces were smaller around the second reduced-diameter cylinder compared to Figure 11(b) because the smaller diameter resulted in the reduced flow velocity around the cylinder.

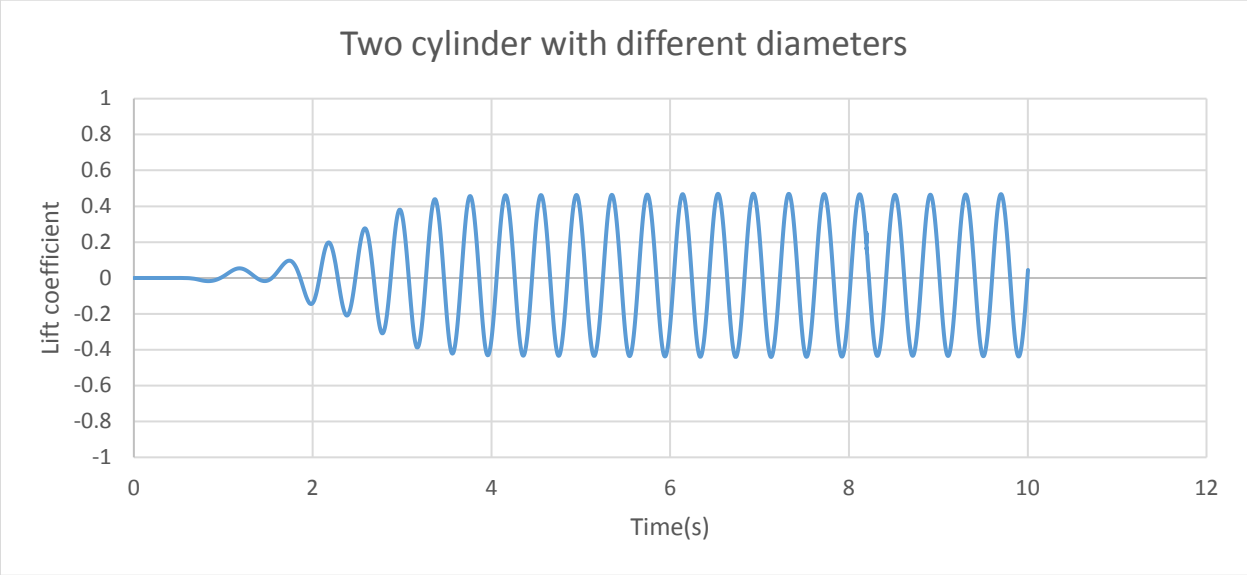

(a) Lift coefficient around the first cylinder (located near the inlet of the channel)

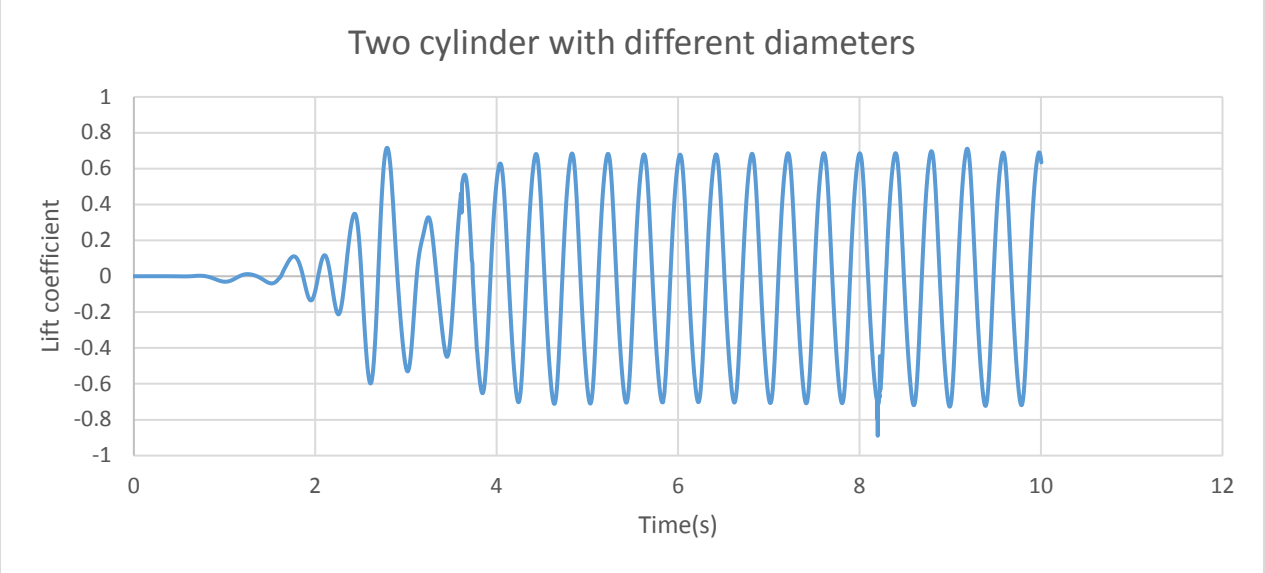

(b) Lift coefficient around the second cylinder (located at the middle of the channel)

Figure 4.9: Lift coefficient around the cylinders in the channel (for the two-different-diameters-cylinder case).

4.3 Drag Coefficient

Drag coefficient was also calculated based on the drag force applied to the cylinders in the channel. The drag force for the rigid cylinder was a constant value (Figure 4.10). For the elastic cylinders, the drag force values oscillated. They were similar around the first cylinder located near the inlet of the channel as shown in Figures 4.11-4.13. The drag force fluctuation amplitude was larger around the second cylinder in the channel compared to the fluctuation level around the first cylinder as displayed in Figures 4.12 and 4.13 due to the larger vortex shedding around the second cylinder as explained in Figures 4.4 and 4.5. The larger vortex shedding resulted in the larger changes of the pressure drop around the second cylinder, which led to the larger drag force fluctuation level. The absolute values of the drag coefficients were similar for both cases (the same-diameter-cylinder case and the reduced-diameter-cylinder case) as shown in Figures 4.12(b) and 4.13(b).

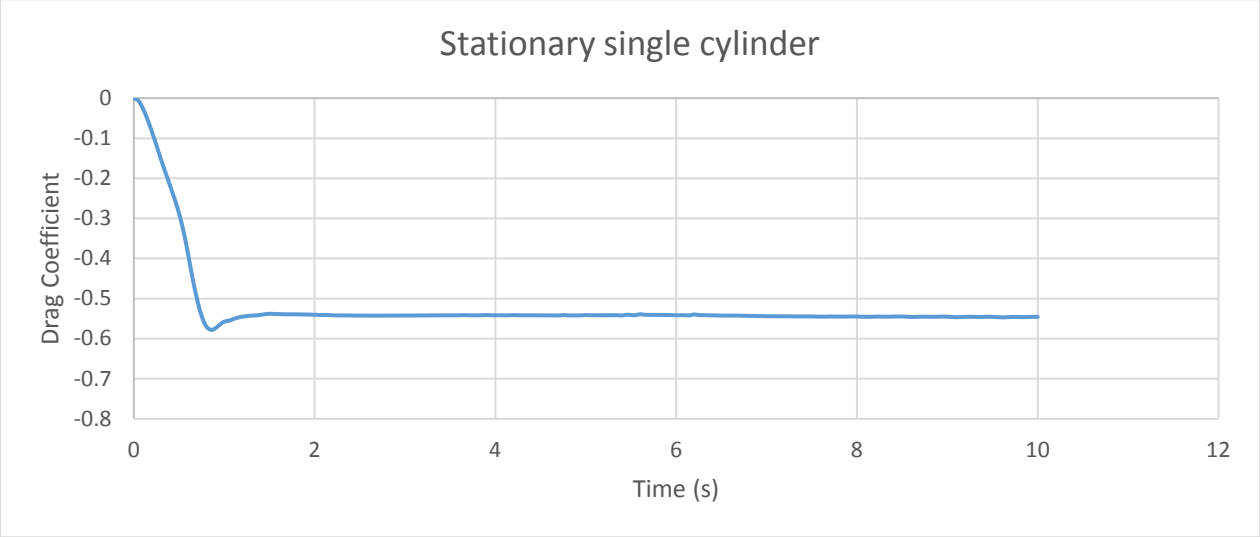

Figure 4.10: Drag coefficient around the cylinder in the channel (for the rigid single cylinder case)

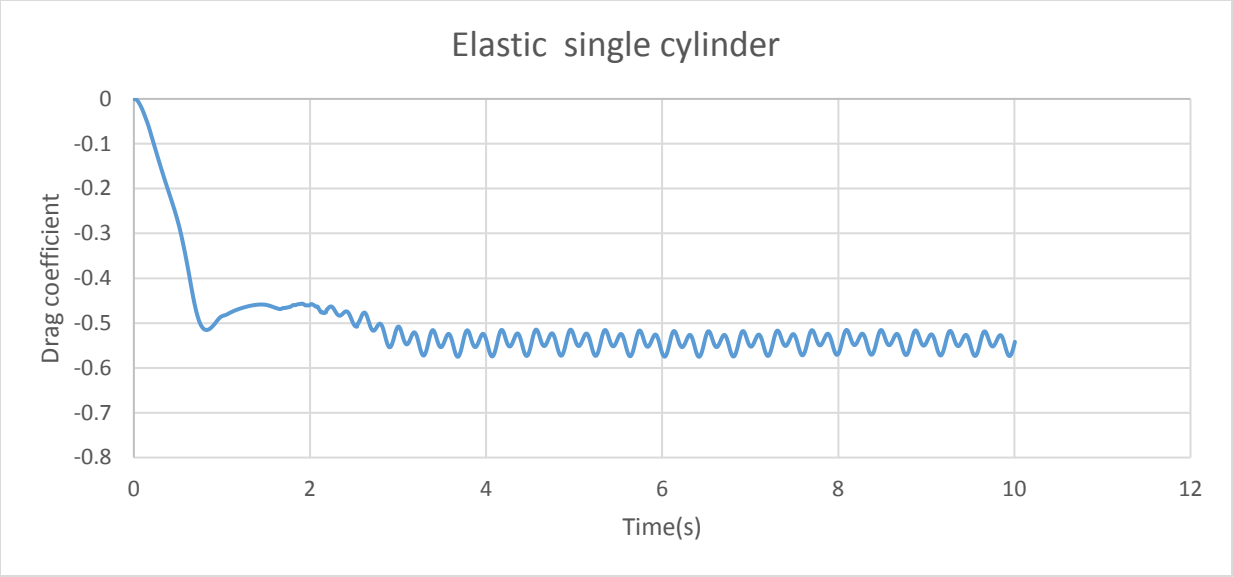

Figure 4.11: Drag coefficient around the cylinder in the channel (for the elastic single cylinder case)

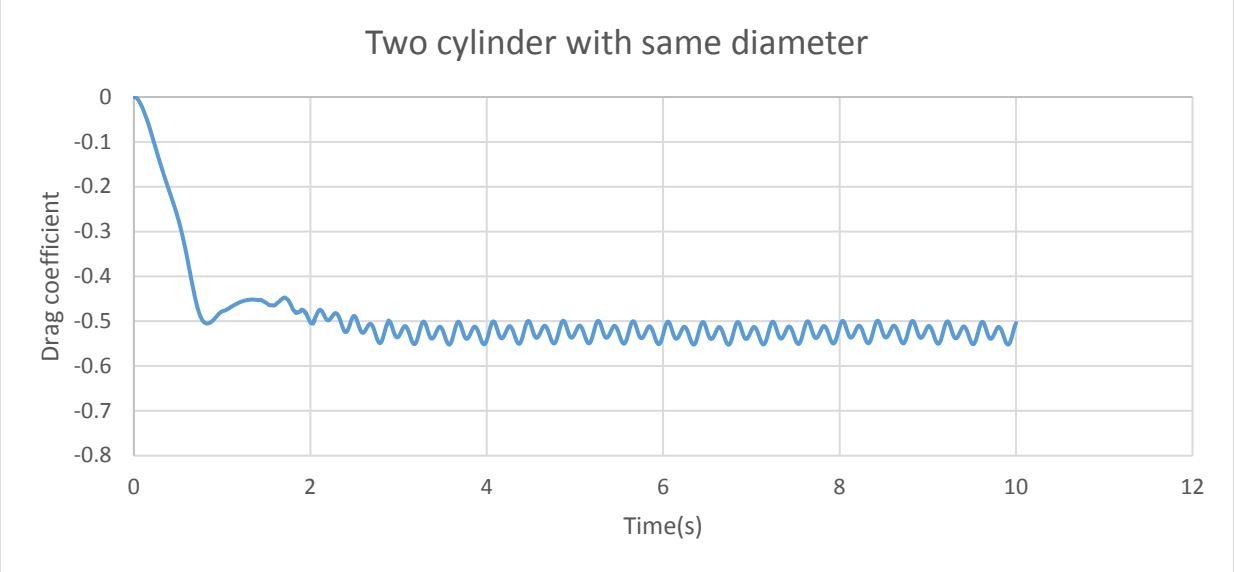

(a) Drag coefficient around the first cylinder (located near the inlet of the channel)

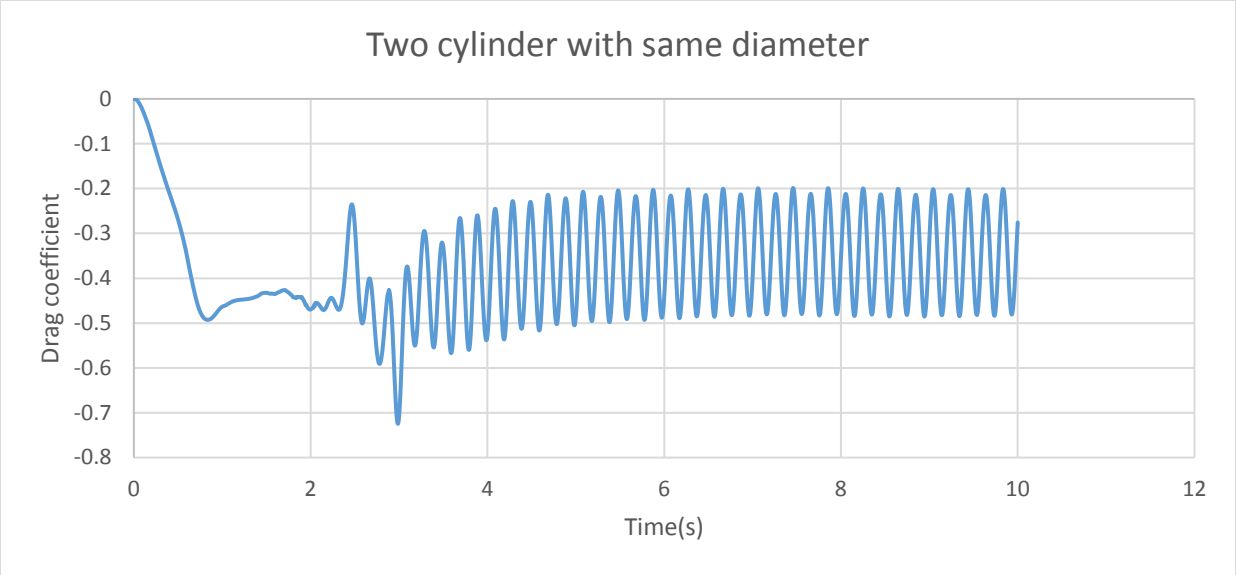

(b) Drag coefficient around the second cylinder (located at the middle of the channel)

Figure 4.12: Drag coefficient around the cylinders in the channel (for the two-same-diameter-cylinder case).

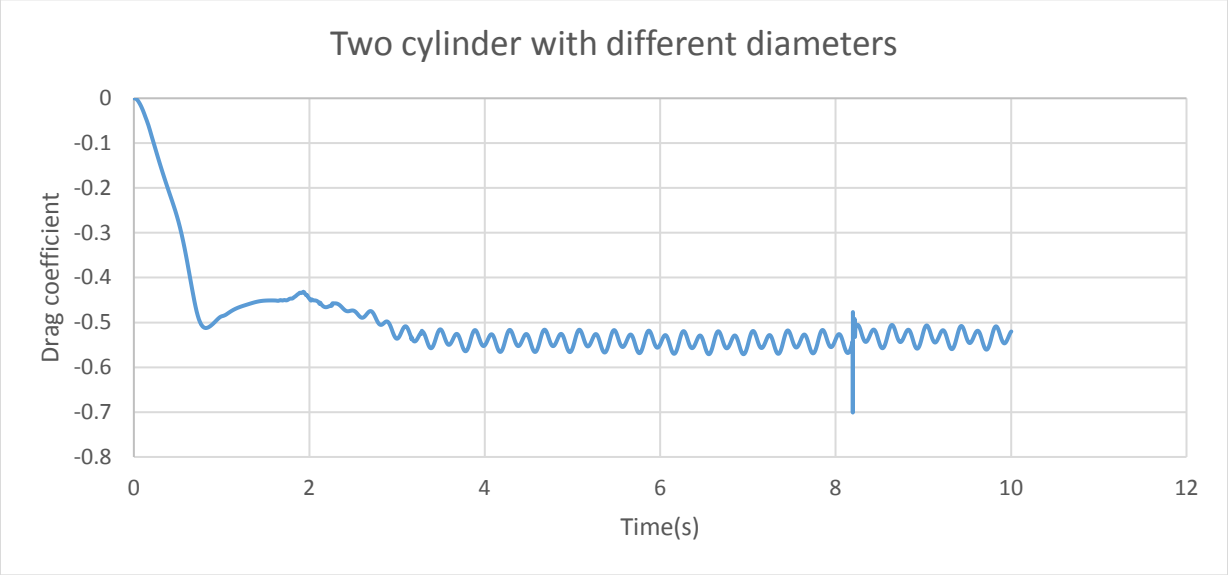

(a) Drag coefficient around the first cylinder (located near the inlet of the channel)

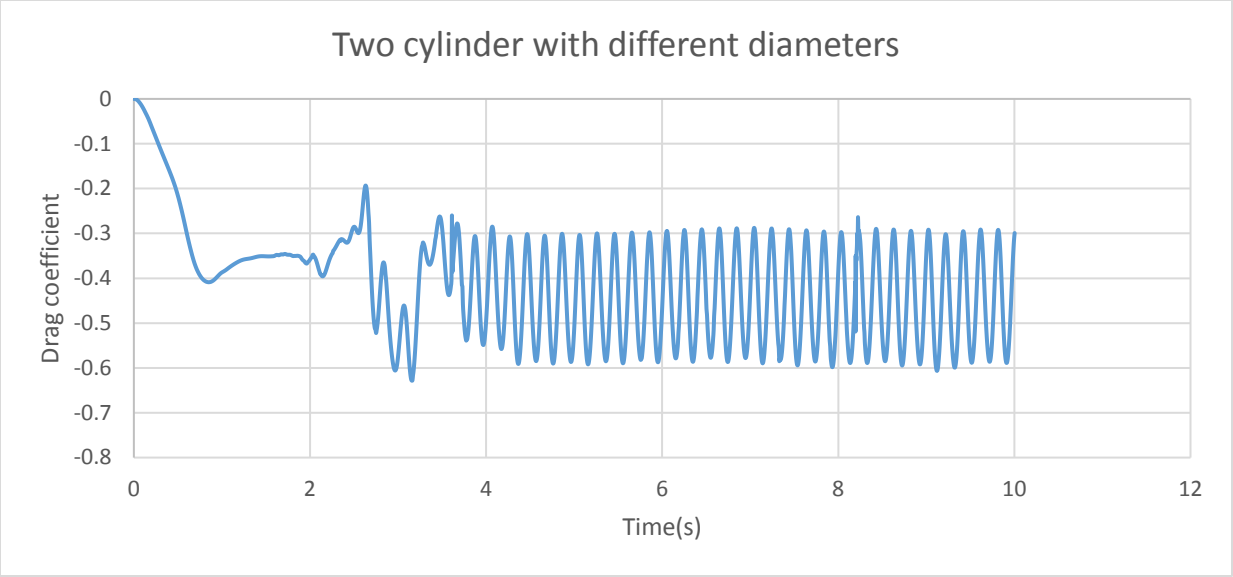

(b) Drag coefficient around the second cylinder (located at the middle of the channel)

Figure 4.13: Drag coefficient around the cylinders in the channel (for the two-different-diameters-cylinder case).

4.4 Displacement of the Cylinder

Figure 4.14 shows the Z-direction displacement at the center point of the elastic cylinder, where the largest displacement occurred. From Figure 4.14, the average displacement at the center point was 0.05mm with the oscillating amplitude of 0.21mm. Therefore, the overall displacement was very small in the order of micro.

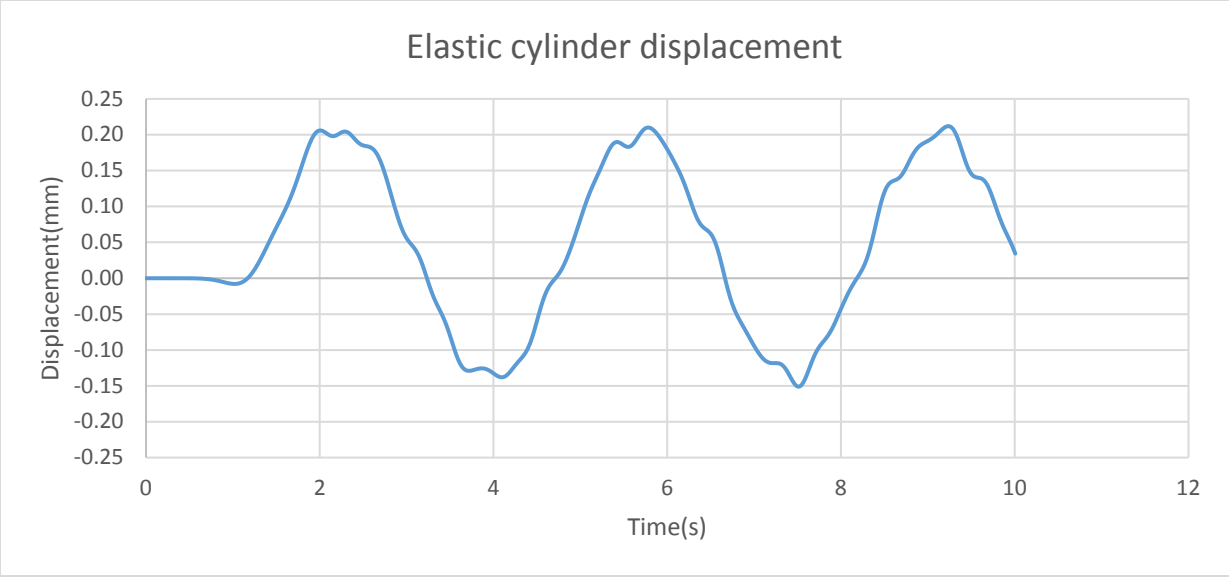

Figure 4.14: Z-axis displacement of the elastic cylinder (mm) in the single-cylinder channel with respect to the time (s)

The frequency spectrum for the displacement, and the lift and drag forces are shown in Figure 4.15. Because the lift force generated around the elastic cylinder was not significant (in the order of 0.1 N) and the mass of the elastic cylinder was large, the overall displacement of the cylinder was very small less than 1mm. Based on the simulation, the frequencies between the displacement and the lift force were not perfectly matched. So the slight vibration of the cylinder may not be caused by the lift force only. Further studies are required to seek the other perturbations in the fluid flow that caused the vibration of the elastic cylinder.

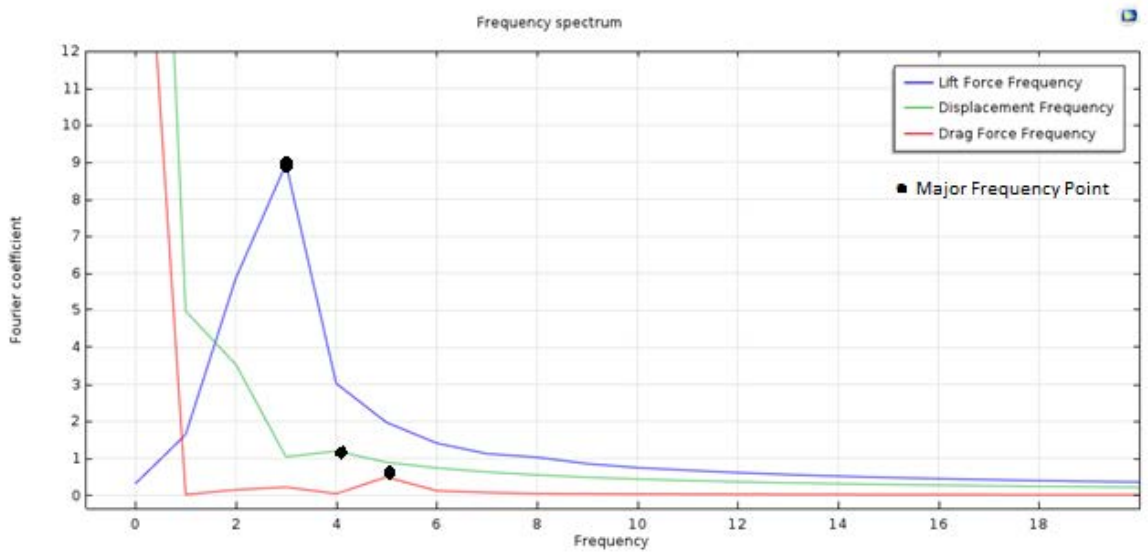

Figure 4.15: The frequency spectrum of the displacement, and the lift and drag forces on the elastic cylinder in one second

4.5 Nusselt Number

4.5.1 Local Nusselt Number

Figure 4.16 showed the local Nusselt number for various channel geometries. The cylinders in the fluid channel would help significantly enhance the local Nusselt number by more than two times compared to the channel without the cylinder. The maximum local Nusselt number occurred at the entrance of the channel. The elastic cylinder could further improve the local Nusselt number compared to the rigid cylinder. The channel with two same-diameter elastic cylinders could maintain the maximum Nusselt number in the entrance region of the channel compared to the other cases due to the vortices generated onto the two cylinders. For the two-different-diameter-cylinder case, the local Nusselt number at the entrance region decreased similarly to that of the elastic cylinder channel because the vortex generation from the reduced diameter cylinder was slightly

weaker than the larger size cylinder (as shown in Figures 9 and 10). The local Nusselt number decreased even faster in the stationary rigid cylinder channel compared to the elastic cylinder cases.

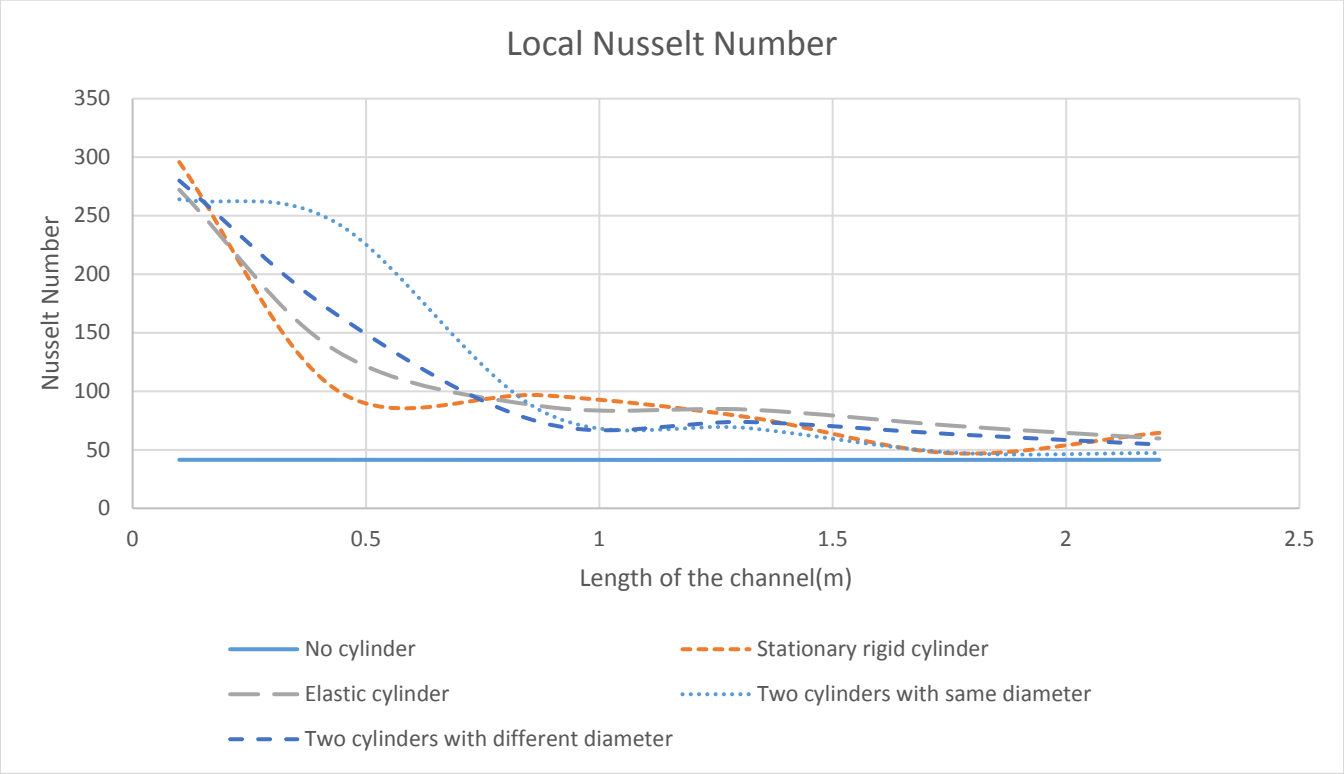

Figure 4.16: Local Nusselt number at Y-Z plane

4.5.2 Average Nusselt Number

From Table 4.1, the average Nusselt Number in the channel with no cylinder was calculated around 50.62. By placing a stationary rigid cylinder, the average Nusselt number was improved by 54.64%. While placing an elastic cylinder into the channel, the average Nusselt number was increased to 93.65 (around 85.0% improvement compared to the no-cylinder channel). For the channel with two elastic cylinders of the same diameter, the average Nusselt Number could be increased from 50.62 to 80.04 with the

improvement of 58.11 %. When it came to the channel with two elastic cylinders of different diameters, the average Nusselt Number increased from 50.62 to 85.72 with the improvement of 69.34%.

Table 4.1: Average Nusselt number in the fluid channels

Type of channel	Average Nusselt Number
Channel with no cylinder	50.62
Channel with stationary rigid cylinder	78.28
Channel with elastic cylinder	93.65
Channel with two cylinders of the same diameter	80.04
Channel with two cylinders of different diameters	85.72

4.6 Temperature

Constant heat rate was applied on the top surface of the channel at 100 W. For the channel with no cylinder, the maximum temperature on the top surface reached to 49.8 ^{0}C as shown in Figure 4.17. For the channel with the stationary rigid cylinder, the maximum temperature on the channel top surface was reduced to 44.8 ^{0}C shown in Figure 4.18. For the elastic single cylinder channel, the maximum temperature on the channel top surface could be further reduced to 41.1 ^{0}C as displayed in (Figure 4.19) because of the increased Nusselt number resulting from the enhanced vortex shedding generated from the elastic cylinder.

By placing two elastic cylinders into the channel (Figure 4.20), the temperature at the top surface was found to increase. The maximum surface temperature was increased to 48.00^{0}C, although the local Nusselt number was higher in the two-cylinder channel.

This was caused by the volume of the second cylinder. The second solid cylinder would occupy some space in the fluid channel, and therefore, reduce a certain amount of fluid for convective heat transfer.

Therefore, by placing the second cylinder with reduced diameter in Figure 4.21, it was observed that the temperature at the top surface of the channel was reduced. The maximum temperature at the top surface was reduced to 42.4^0C. Hence, the reduced volume of the solid cylinder could give more space for convection fluid. Thus, the size of the cylinder is also important for the overall heat transfer performance in the channel.

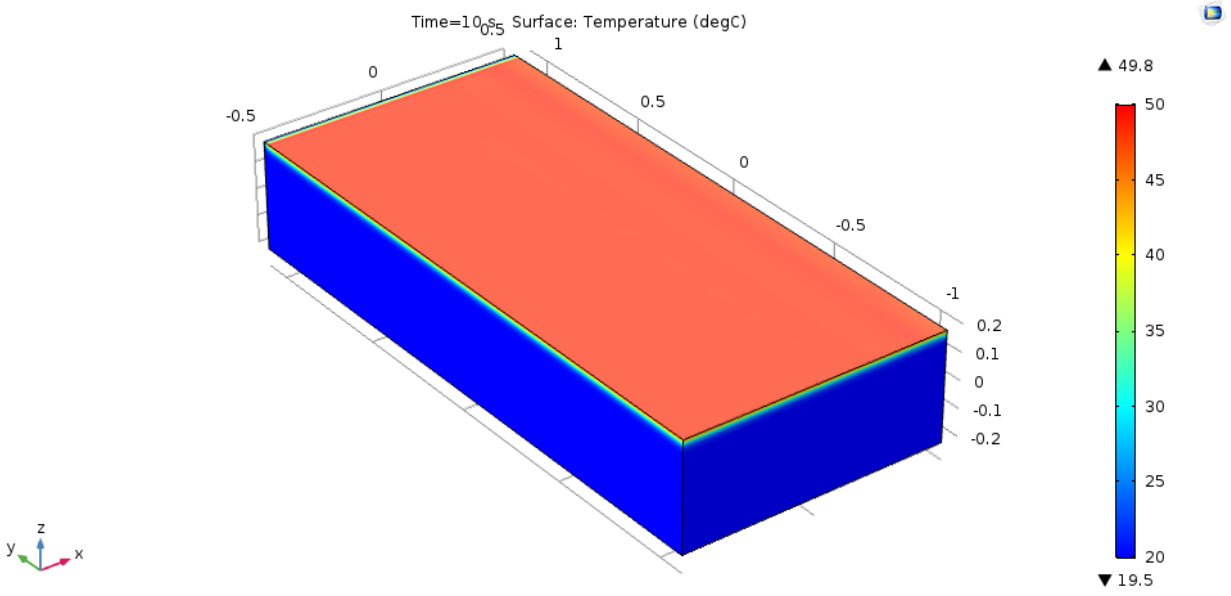

Figure 4.17: Temperature contour of fluid channel without cylinder

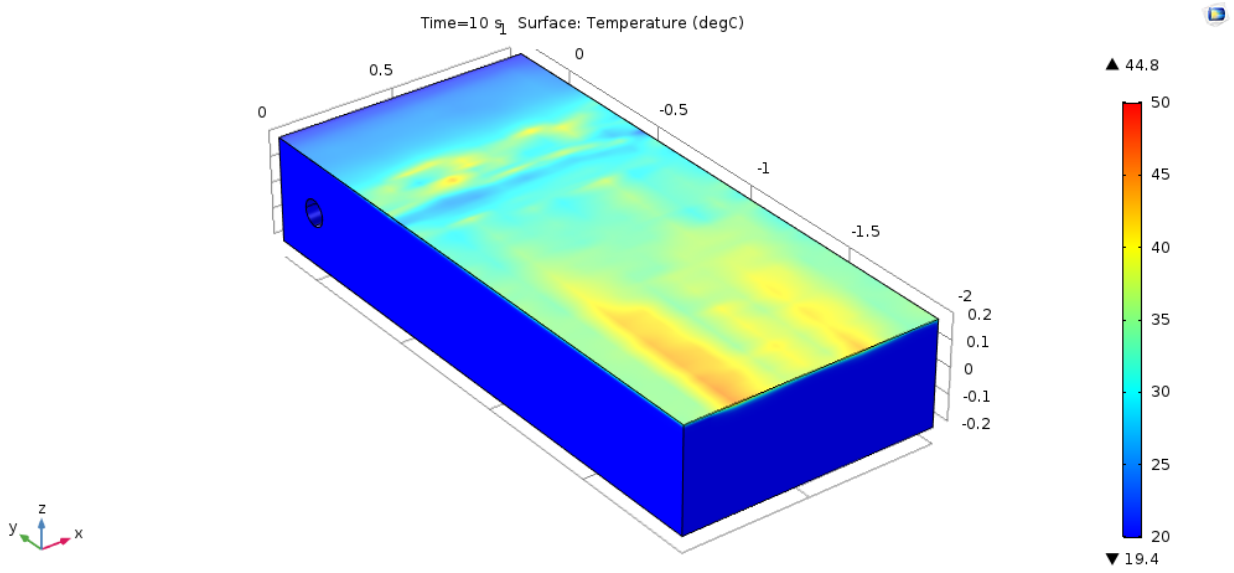

Figure 4.18: Temperature contour of fluid channel with stationary rigid cylinder

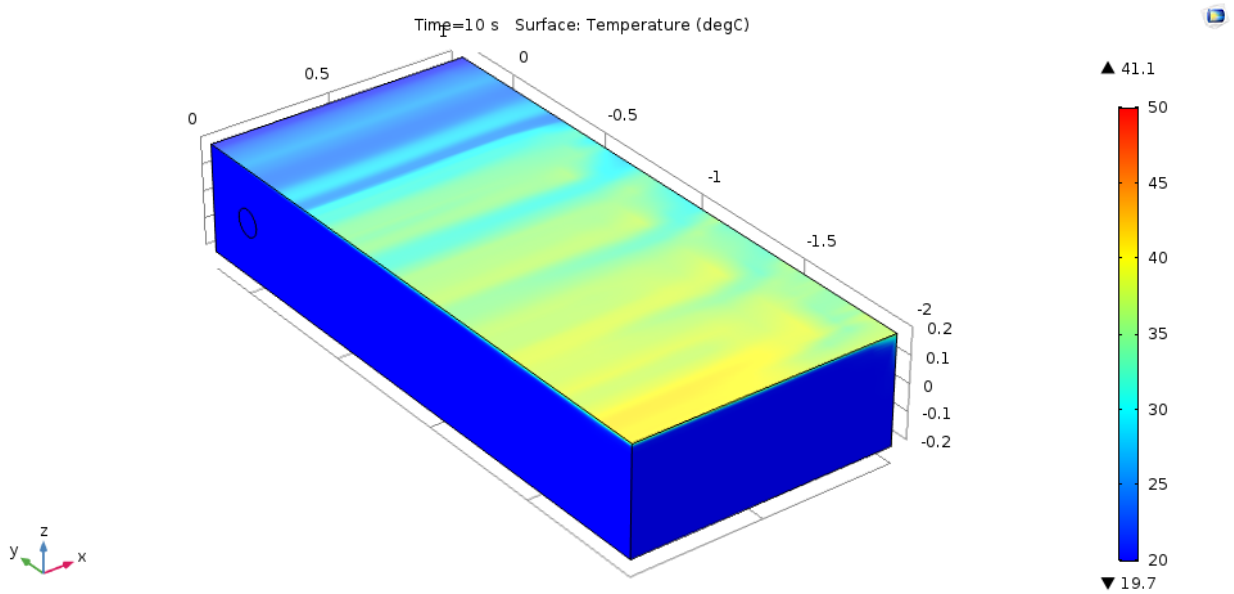

Figure 4.19: Temperature contour of fluid channel with elastic single cylinder

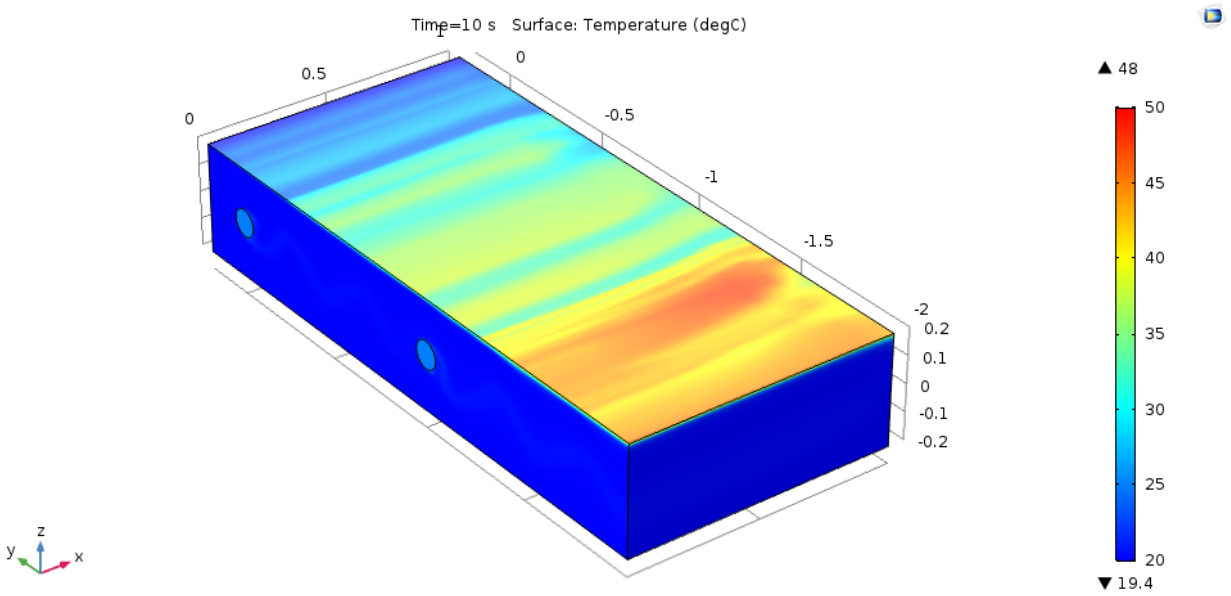

Figure 4.20: Temperature contour of fluid channel with two cylinders of the same diameter

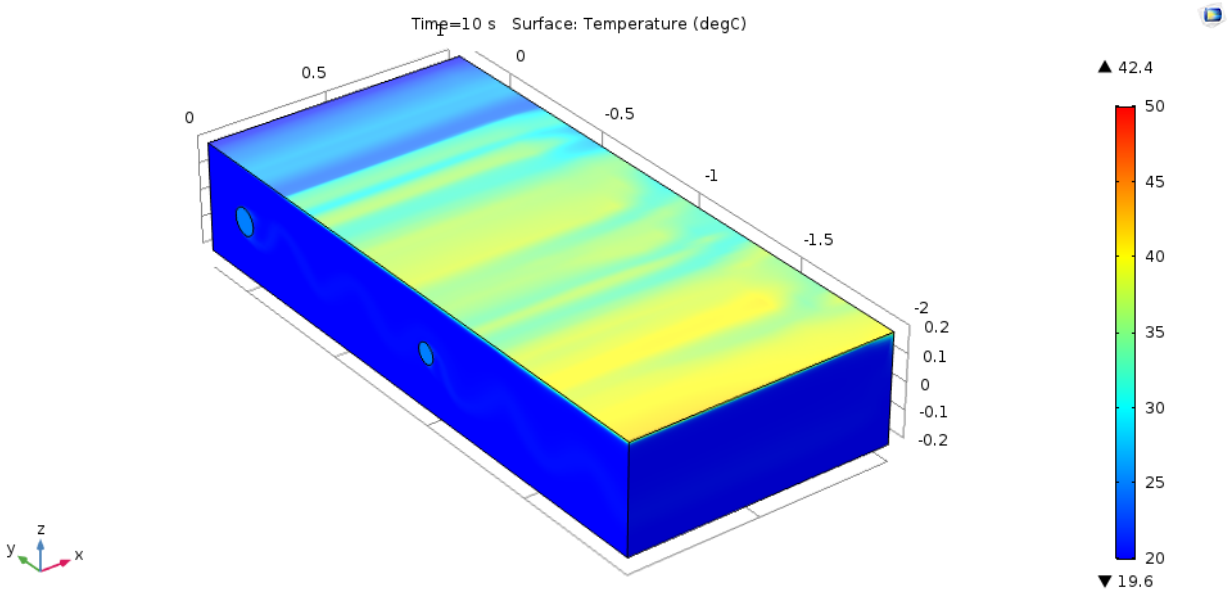

Figure 4.21: Temperature contour of fluid channel with two cylinders of different diameters.

CHAPTER 5

CONCLUSION AND FUTURE WORK

5.1 Conclusion

In this research, the elastic cylinder that utilized vortex-induced vibration was applied to improve the convective heat transfer rates by disrupting the thermal boundary layer. Rigid and elastic cylinders were placed across a fluid channel. The flow-structure interaction increased the disruption of the thermal boundary layer based on the velocity profiles in the fluid channel, and therefore, improved the mixing process at the boundary. This study aimed to improve convective heat transfer rate by increasing the perturbation in the fluid flow through elastic cylinders. A three-dimensional numerical model was constructed to simulate the effects of different flow channel geometries, including the channel with a stationary rigid cylinder, channel with elastic cylinder, channel with two elastic cylinders of the same diameter, and the channel with two elastic cylinders of different diameters. Through the numerical simulations, the channel maximum wall temperature was found to be reduced by approximately 10% through introducing a stationary rigid cylinder and by around 17% through introducing an elastic cylinder in the channel compared with the channel without the cylinder. Furthermore, the channels with two-cylinder conditions have also been studied in the current research. The additional elastic cylinder in the fluid channel only reduced the wall temperature by 3% compared to the channel without the cylinders because the volume of the second cylinder could occupy some spaces, and therefore, the reduction of the temperature was less on the top of the channel surface. Through reducing the diameter of the second cylinder by

25%, the effect of the convection heat transfer would be increased and the maximum channel wall temperature would be reduced by around 15%.

By introducing cylinders in the channel flow, the average Nusselt number in the channel could be increased by 55% with the insertion of a rigid cylinder, by 85% with the insertion of an elastic cylinder, by 58% with the insertion of two cylinders of the same diameter, and by approximately 70% with the insertion of two cylinder of different diameters (the second cylinder diameter was reduced by 25%) compared to the channel with no cylinder.

Therefore, using elastic cylinders, can enhance the convective heat transfer performance without the external power source requirements. Moreover, when multiple vibrating cylinders were considered in the channel, the sizes of the cylinders were critical. The proper cylinder sizes should be evaluated and determined to maximize the overall convective heat transfer rate.

5.2 Future Work

In the future, we can look into various parameters, such as the dimensions of the cylinder, the structure of the cylinder (e.g., attaching some fin structures to the cylinder, etc.), the mechanical properties of cylinder material, etc., to study how these parameters of the elastic cylinder would affect and improve the convective heat transfer in the channel. Moreover, other perturbation factors in the fluid flow will also be investigated for the further studies on the flow-structure interaction. Furthermore, we will also establish and conduct experiments on flow-induced vibration in a wind channel to

experimentally investigate the convective heat transfer enhancement by elastic cylinders as well as verify our simulation model.

REFERENCES

[1] Jacobi, A. M., “Heat Transfer Surface Enhancement through the Use of Longitudinal Vortices: A Review of Recent Progress”. Experimental thermal and fluid science., Vol.11, (1995):295-309.

[2] Edwards, F. J., and Alker, C. J. R., “The Improvement of Forced Convection Surface Heat Transfer Using Surface Protrusions in the Form of (A) Cubes and (B) Vortex Generators”, Heat Transfer 1974, Proc Fifth Int. Heat Transfer Conf., Vol. 2, (1974): 244-248.

[3] Johnson, T. R., and Joubert, P. N., “The Influence of Vortex Generators on Drag and Heat Transfer from a Circular Cylinder Normal to an Airstream”, J. Heat Transfer, 91, (1969):91-99.

[4] Kataoka, K., Doi, H., and Komai, T., “Heat/Mass Transfer in Taylor Vortex Flow with Constant Axial Flow Rates”, Int. J. Heat Mass Transfer, 20, (1977):57-63.

[5] Sedney, R., “A Survey of the Effects of Small Protuberances on Boundary-Layer Flows”, A/AA J. 11, (1973):782-792.

[6] Baker, C. J., “The Laminar Horseshoe Vortex”, J. Fluid Mech., 95, (1979):347-367.

[7] Cheng, L., Zhou, Y., Zhang, M.M., “Perturbed interaction between vortex shedding and induced vibration”, Journal of Fluids and Structures 17, (2003): 887–901.

[8] Fujarra, A.L.C., Fleming, F., Williamson, C, H, K., “The Vortex-induced vibration of a flexible cantilever”, Journal of Fluids and Structures 15, (2001):651-658.

[9] Griffinth et al., “Vortex shedding and three-dimensional behavior of flow past a cylinder confined in a channel”, Journal of Fluids and Structures 27, (2011):855–860.

[10] Huisseune et al., “Performance Enhancement of a louvered fin heat exchanger by using delta winglet vortex generators”, International Journal of Heat and Mass Transfer 56, (2013):475–487.

[11] He et al., “Numerical study of heat transfer enhancement by punched winglet-type vortex generator arrays in fin-and-tube heat exchangers”, International Journal of Heat and Mass Transfer 55,21-22, (2012):5549-5558.

[12] Jagannatha et al., “Interactive flow behavior and heat transfer enhancement in a microchannel with cross-flow synthetic Jet”, International Journal of Emerging Multidisciplinary Fluid Sciences. 2(1): pages 27-43.

[13] Youmin et al., “Enhancing heat transfer in air cooled heat sinks using piezo-electrically driven agitators and synthetic Jets”, International Journal of Heat and Mass Transfer 68, (2014):184-193.

[14] Li Hung-Yi., Chen Kuan-Ying., “Thermal performance of plate-fin heat sinks under confined impinging jet conditions”, International Journal of Heat and Mass Transfer 50, (2007):1963–1970.

[15] Chao et al., “Thermal Performance of a Plate-fin Heat Sink with a Shield”, IEEE 3rd International Conference on Communication Software and Networks (ICCSN),10, (2011):1109/ICCSN.6014886.

[16] Yamamoto et al., “Numerical simulations of vortex induced vibration on flexible cylinders”, Journal of fluid and structures. Vol 19, (2004):467-489.

[17] Williamson, C.H.K. and R. Govardhan., “Vortex-induced Vibrations”. Annual Review of Fluid Mechanics,36(1), (2004):413-455.

[18] singha et al., “Flow past a circular cylinder between parallel walls at low Reynolds numbers”, ocean engineering, Volume 37, (2010): Issues 8–9, P. 757–769.

[19] Fu, W.-S., and B.-H. Tong, “Numerical investigation of heat transfer characteristics of the heated blocks in the channel with a transversely oscillating cylinder”, International Journal of Heat and Mass Transfer, (2004): 47(2),341-351.

[20] Bayram et al., “Heat transfer enhancement in a slot channel via a transversely oscillating adiabatic circular cylinder”, International Journal of Heat and Mass Transfer, (2010): 53: p.626–634.

[21] Beskok Ali et al., “Heat transfer enhancement in a straight channel via a rotationally oscillating adiabatic cylinder”, International Journal of Thermal Sciences 58, (2012): P:61-69.

[22] Shi et al., “Heat transfer enhancement of channel flow via vortex induced vibration of the flexible cylinder”, ASME 2014 4th Joint US-European Fluids Engineering Division Summer Meeting, (2014): Vol 1B, ISBN 978-0-7918-4622-3.

[23] Bergles et al., “Bibliography on Augmentation of Convective Heat and Mass Transfer II,” Heat Transfer Laboratory Report *HTL-31*, ISU-ERI-Ames-84221, (December 1983): Iowa State University.

[24] Leal et al.,” An overview of heat Transfer enhancement methods and new perspectives: Focus on active methods using electroactive materials”, International Journal of mass and heat transfer, volume 61, (June 2013):505-524.

[25] Kakac et al., “Review of convective heat transfer enhancement with nanofluids”, Int. J. Heat Mass Transfer 52 (13–14), (2009): 3187–3196.

[26] Bontemps et al., “Echangeur de chaleur: intensification des échanges thermiques”, Techniques de l’ingénieur (1994):

[27] M. Miscevic et al., “Experiments on flows, boiling and heat transfer in porous media: emphasis on bottom injection”, Nucl. Eng. Des.236 (19–21) (2006):2084–2103.

[28] A.S. Dalkilic, S. Wongwises, “Intensive literature review of condensation inside

smooth and enhanced tubes”, Int. J. Heat Mass Transfer 52 (15–16) (2009): 3409–3426.

[29] Cavallini et al., “A new computational procedure for heat transfer and pressure drop during refrigerant condensation inside enhanced tubes”, J. Enhanced Heat Transfer 6 (6) (1999): 441–456.

[30] Miyara et al., “Effects of fin shape on condensation in herringbone microfin tubes”, Int. J. Refrig. 26 (4) (2003):417–424.

[31] Sheikholeslami et al., “Review of heat transfer enhancement methods: Focus on passive methods using swirl flow devices”. Renewable and sustainable energy reviews. Volume 49, (September 2015): P:444-469.

[32] Kumar et al., “Investigation of twisted tape inserted solar water heaters heat transfer”, friction factor and thermal performance results. Renew Energy, (2000): (19) 379–98.

[33] Promvonge,P.”Heat transfer behaviors in round tube with conical ring inserts”, Energy Conversion and Management. Volume 49, Issue 1, (January 2008): 8-15.

[34] Promvonge et al., “Heat transfer in a circular tube fitted with free- spacing snail entry and conical-nozzle turbulators”. International Communications in Heat and Mass Transfer, Volume 34, Issue 7, (August 2007): Pages 838-848.

[35] Gunes et al., “Heat transfer enhancement in a tube with equilateral triangle cross-sectioned coiled wire inserts”, Experimental Thermal and Fluid Science, Volume 34, Issue 6, (September 2010): 684-691.

[36] Johnson et al., “The influence of Vortex Generators on Drag and Heat Transfer from a Circular Cylinder normal to an Airstream”, J. Heat Transfer, 91, (1969):91-99.

[37] Shakaba et al., “Longitudinal Vortices Imbedded in Turbulent Boundary Layers. Part1.single Vortex, J. Fluid Mechanics, 155, (1983): 37-57.

[38] Knupp, P.M, “Winslow Smoothing on Two-Dimensional Unstructured Meshes”, Engineering with Computers, (September 1999): Volume 15, Issue 3, 263-268.

[39] Bearman et al., **“**A model equation for the transverse forces on cylinders in oscillatory flows”, Applied Ocean Research, 6 (1984):166-172.